materials design

Precision at Scale with Machine-Learned Potentials

Volker Eyert and Jörg-Rüdiger Hill

December 10-12, 2025

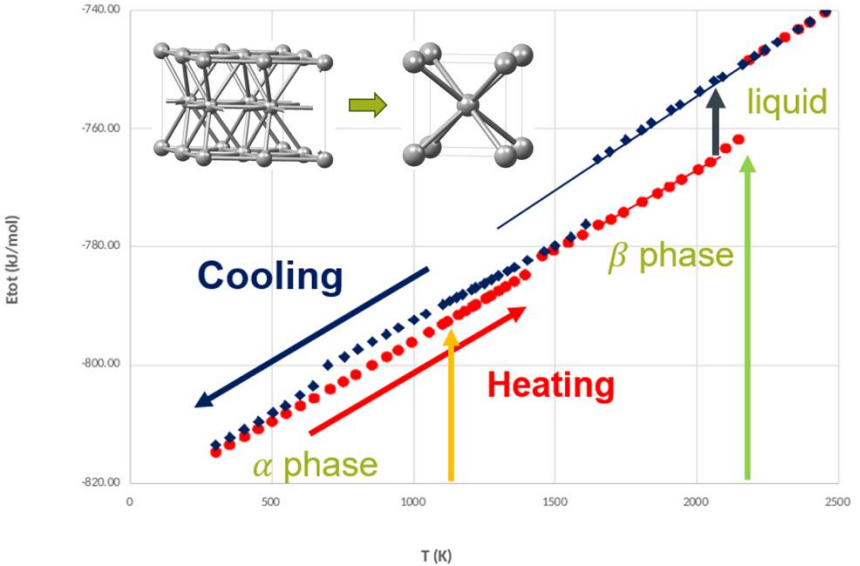

Materials Design Webinar Series

- Each session runs several times to accommodate schedules
  - Share the webinar series with your colleagues!
  - Registration details http://www.materialsdesign.com/webinars
- We will be recording this webinar
  - Watch any of our earlier webinars anytime
  - We will post upcoming webinars on the webinar page
- Vote for the next webinar topic!
  - Take a 2 minutes brief survey at the end of the webinar!
- Audio issues
  - Log out and log back in again
  - Check your audio output
  - Google Chrome (most recent 2 versions) Mozilla Firefox (most recent 2 versions) Apple Safari (most recent 2 versions) Microsoft Edge (most recent 2 versions)

materials design

GoTo Webinar Interface – Please Ask Questions!

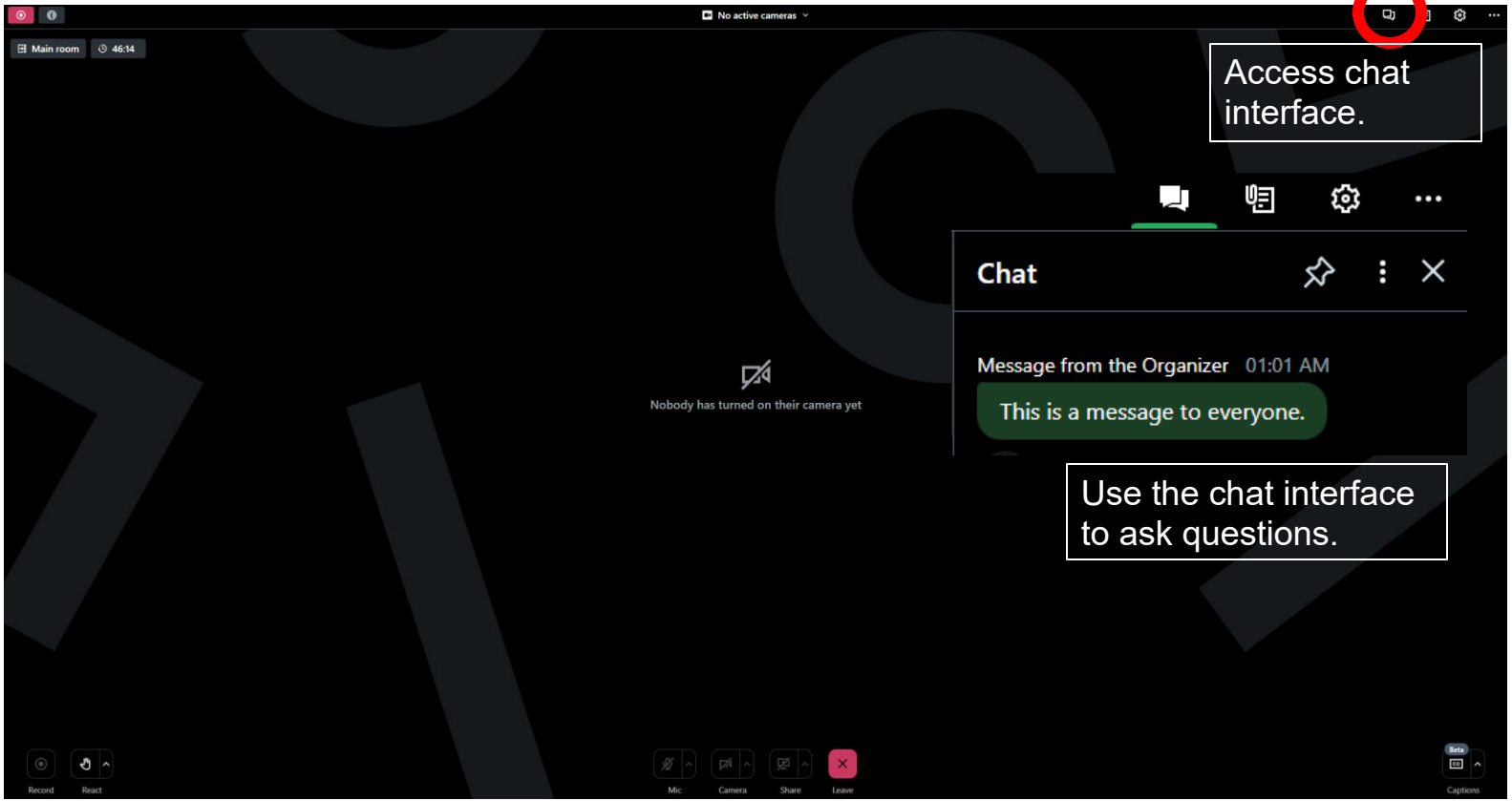

materials design

Webinar Speakers

Katherine Hollingsworth

Dr. Volker Eyert

Dr. Jörg-Rüdiger Hill

materials design

Precision at Scale with Machine-Learned Potentials

Volker Eyert and Jörg-Rüdiger Hill

December 10-12, 2025

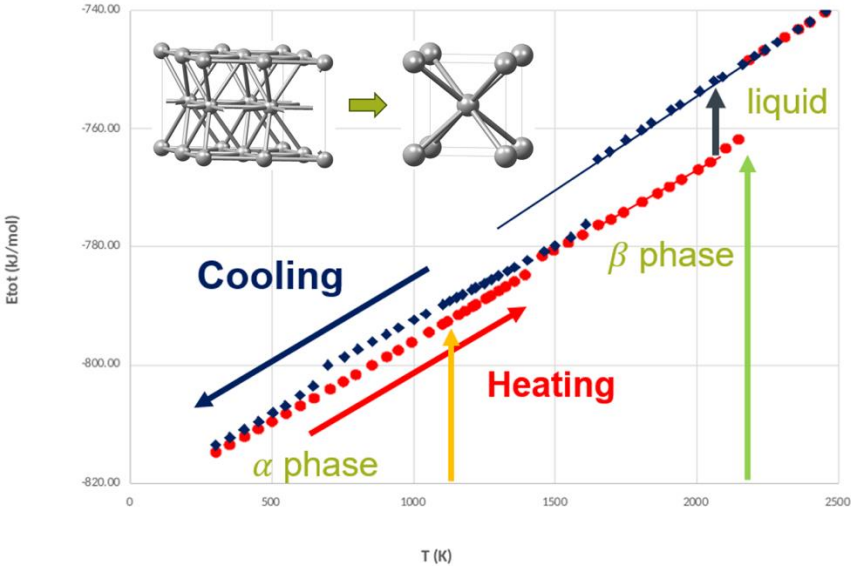

Corrosion

The global cost of corrosion is estimated to be US$2.5 trillion, which is equivalent to 3.4% of the global GDP. Numerous industries are affected including:

1) Energy:
   - Water-cooled reactors
     - Corrosion of fuel cells is one of the major life-limiting degradation mechanism in these reactors

2) Energy:
   - Oil & Gas
     - Corroding pipelines and various equipment in Oil and gas

3) Automotive:
   - Magnesium alloys have been used due to their mechanical properties and castability but they have poor corrosion resistance.

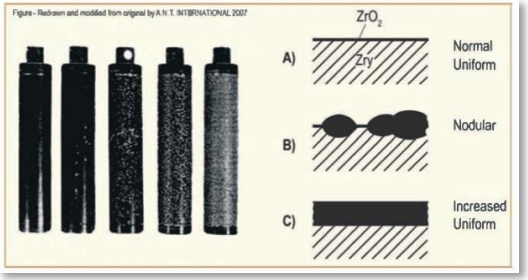

R. Adamson et al., *Corrosion mechanisms in zirconium alloys*, *ZIRAT12 Special Topic Report* (2007)

M. Askari, M. Aliofkhazraei, and S. Afroukhteh, J. Nat. Gas Sci. Eng. **71**, 102971 (2019) https://doi.org/10.1016/J.JNGSE.2019.102971

materials design

Hydrogen Embrittlement of Zirconium Alloys

95% Zr; Sn, Nb, Fe, O can be present

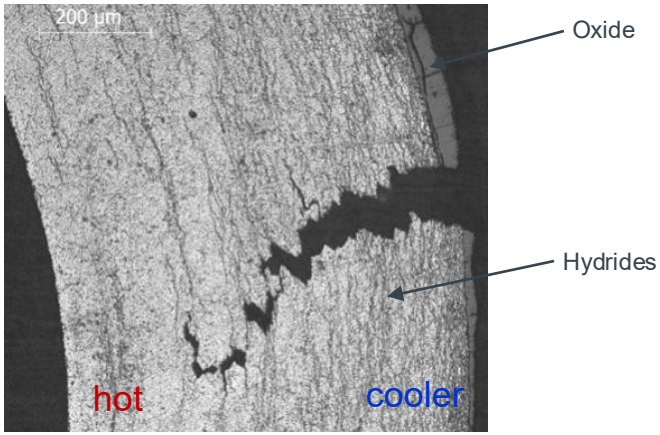

Cross section of fuel rod, Zr alloy

Corrosion of Zr alloys:

$$Zr + 2H_2O \rightarrow ZrO_2 + 4H$$

$$2H \rightarrow H_2$$

$$2H + Zr \rightarrow ZrH_2$$

embrittles

materials design

Bridging time and length scales

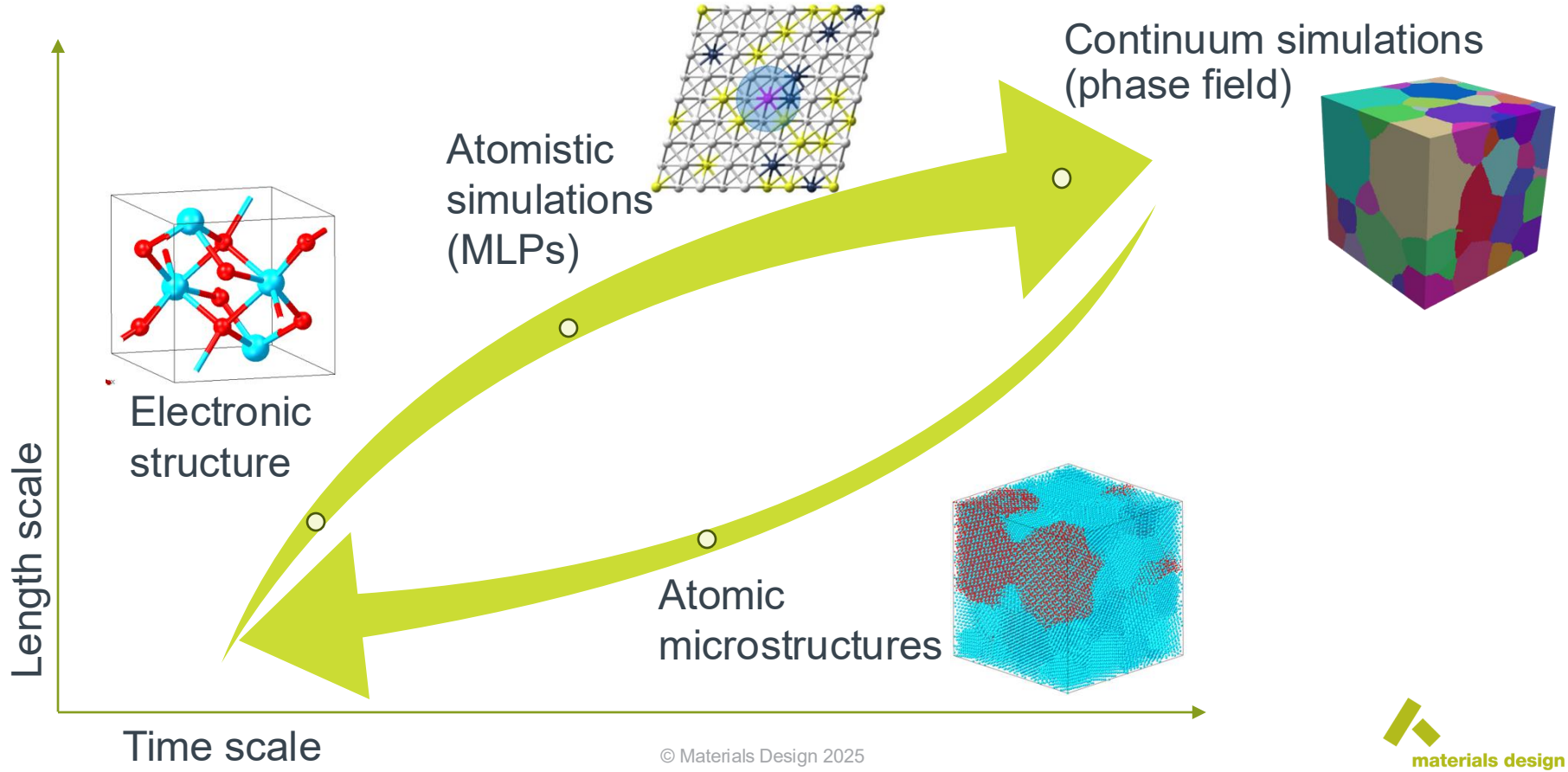

materials design

Back in 2020

The vision

- Creation of an Advanced Materials Simulation Engineering Tool for reliable large-scale simulations of thermomechanical and chemical properties of engineering materials

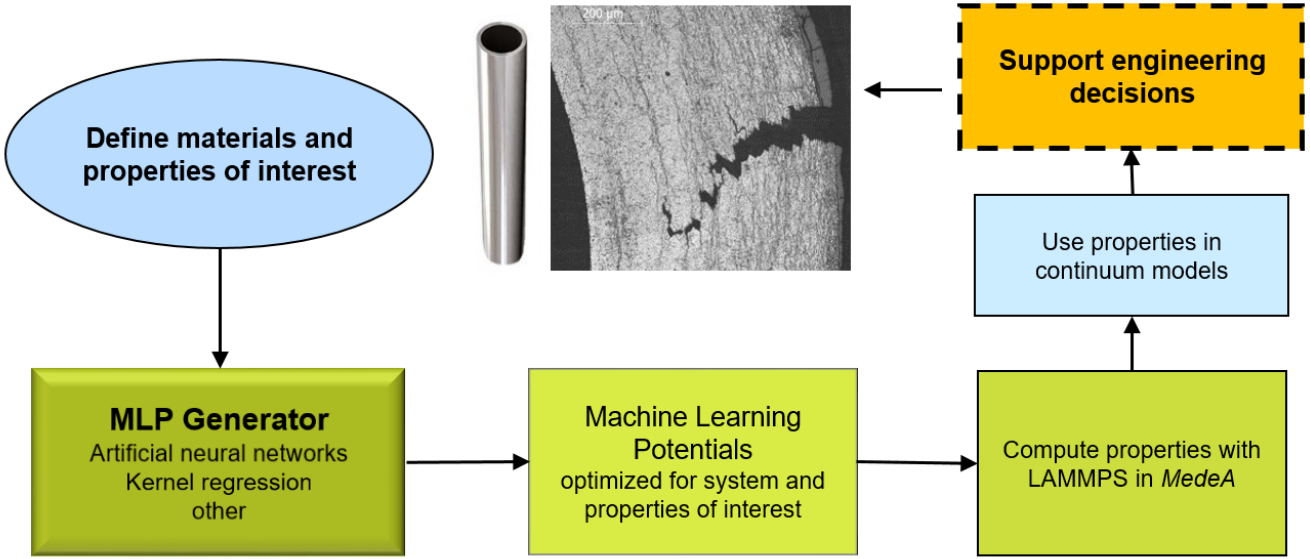

materials design

Back in 1998

4596 *J. Phys. Chem. A* **1998,** *102,* 4596−4605

Representation of Intermolecular Potential Functions by Neural Networks

Helmut Gassner,[†] Michael Probst,[*,†] Albert Lauenstein,[‡] and Kersti Hermansson[‡]

Institute of General and Inorganic Chemistry, Innsbruck University, Innrain 52a, A-6020 Innsbruck, Austria, and Inorganic Chemistry, The Ångström Laboratory, Uppsala University, Box 538, S-75121 Uppsala, Sweden

Received: July 8, 1997; In Final Form: March 17, 1998

We have investigated how a neural network representation of intermolecular potential functions can be used to elevate some of the problems commonly encountered during fitting and application of analytical potential functions in computer simulations. For this purpose we applied feed-forward networks of various sizes to reproduce the three-body interaction energies in the system $H_2O-Al^{3+}-H_2O$. In this highly polarizable system the three-body interaction terms are necessary for an accurate description of the system, and it proved difficult to fit an analytical function to them. Subsequently we performed Monte Carlo simulations on an Al^{3+} ion dissolved in water and compared the results obtained using the neural network type potential function with those using a conventional analytical potential. The performance and results of our calculations lead to the conclusion that, for suitable systems, the advantages of a neural network type representation of potential functions as a model-independent and "semiautomatic" potential function outweigh the disadvantages in computing speed and lack of interpretability.

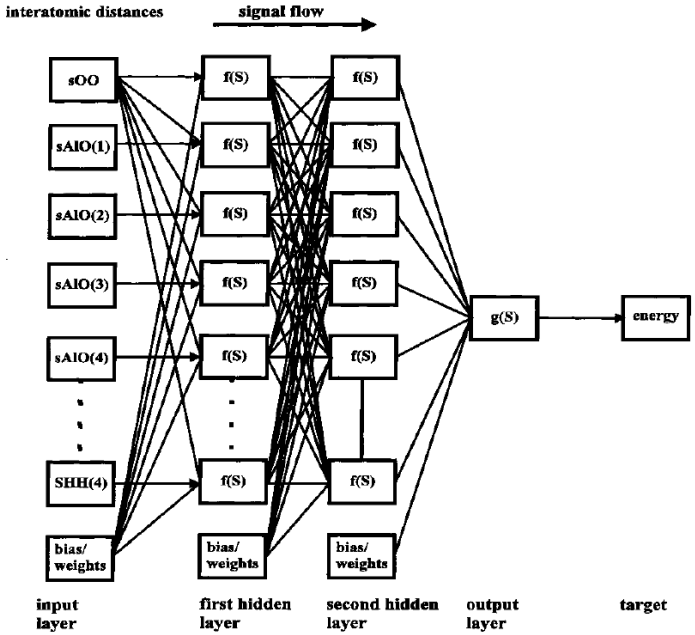

Figure 1. Architecture of the feed-forward network. The input consists of a vector of interatomic distances which are processed to calculate the energy.

materials design

The 2000s and 2010s

- S. Manzhos and T. Carrington, *A random-sampling high dimensional model representation neural network for building potential energy surfaces*, J. Chem. Phys. **125**, 084109 (2006).
- J. Behler and M. Parrinello, *Generalized Neural-Network Representation of High-Dimensional Potential-Energy Surfaces*, Phys. Rev. Lett. **98**, 146401 (2007).
- A. P. Bartók, M. C. Payne, R. Kondor, and G. Csányi, *Gaussian Approximation Potentials: The Accuracy of Quantum Mechanics, without the Electrons*, Phys. Rev. Lett. **104**, 136403 (2010).
- A. P. Thompson, L. P. Swiler, C. R. Trott, S. M. Foiles, and G. J. Tucker, *Spectral neighbor analysis method for automated generation of quantum-accurate interatomic potentials*, J. Comp. Phys. **285**, 316 (2015).
- A. V. Shapeev, *Moment Tensor Potentials: A Class of Systematically Improvable Interatomic Potentials*, Multiscale Model. Simul. **14**, 1153 (2016).
- R. Drautz, *Atomic cluster expansion for accurate and transferable interatomic potentials*, Phys. Rev. B **99**, 014104 (2019); Phys. Rev. B **100**, 249901(E) (2019).

materials design

Agenda

- Motivation
- MLP Product Line
- Selected Applications
  - Equilibrium properties
  - Phase transitions
  - Nanoparticles
  - Surface Interactions
  - Zeolites
- Concluding Remarks

Acknowledgements

- All colleagues at Materials Design, especially
  - David Reith, Leonid Kahle, Mikael Christensen, Marthe Bideault, Garrett Tow, Shubham Pandey, Michele Kotiuga, Clint Geller, Marianna Yiannourakou, and Erich Wimmer
- Customers of Materials Design, especially
  - Jonathan Wormald (Naval Nuclear Laboratory)
  - The machine-learned potential (MLP) work was funded by the Advanced Materials Simulation Engineering Tool (AMSET) project sponsored by NNL
- Science and technology partners, especially
  - Ralf Drautz, Matous Mrovec, Yury Lysogorskiy, Anton Bochkarev, Minaam Qamar

materials design

MLPs in *MedeA*

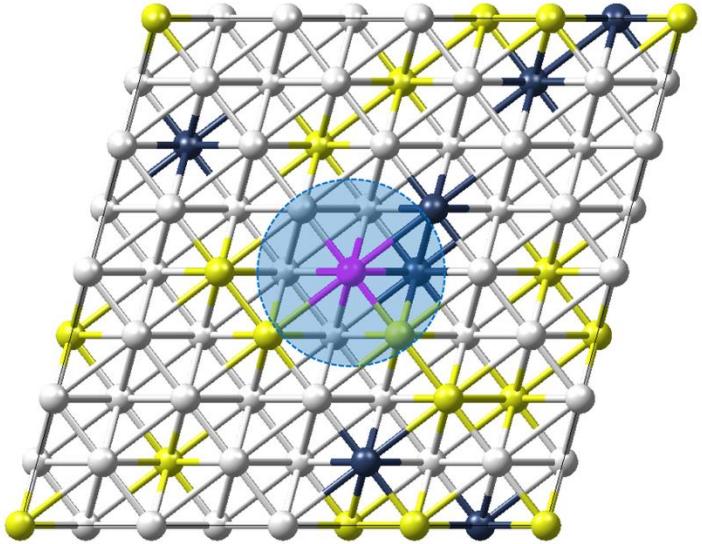

MedeA MLP Generator

Collection of tools to generate MLPs from user-created training sets for subsequent use with *MedeA* LAMMPS

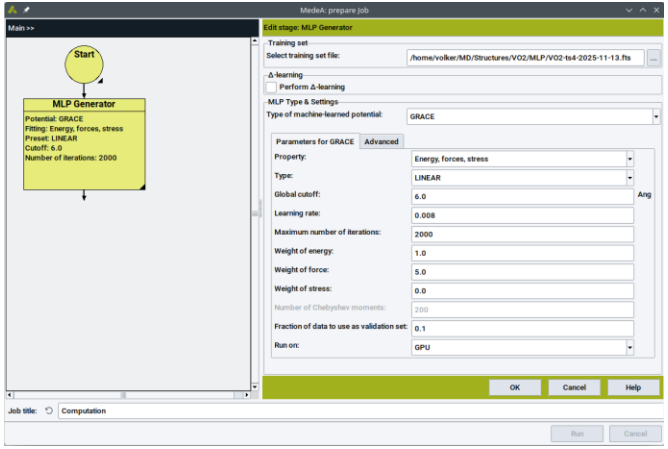

Spectral Neighbor Analysis Potential (**SNAP/qSNAP**)

- A. Thompson and M. Wood
- FitSNAP code by Sandia group

Neural Network Potential (**NNP**)

- J. Behler and M. Parrinello
- n2p2 code by A. Singraber, Vienna

Atomic Cluster Expansion (**ACE**) and Graph ACE (**GRACE**)

- R. Drautz, Y. Lysogorskiy, A. Bochkarev, and M. Mrovec
- PACEMAKER/GRACEMAKER code by ICAMS group

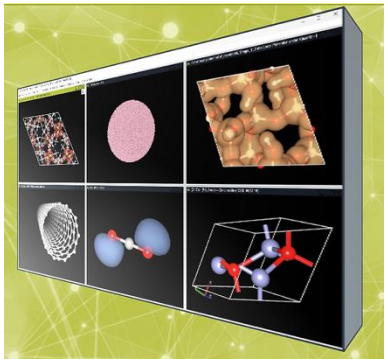

materials design

MedeA MLPs

Collection of pre-trained MLPs ready to use with *MedeA* LAMMPS

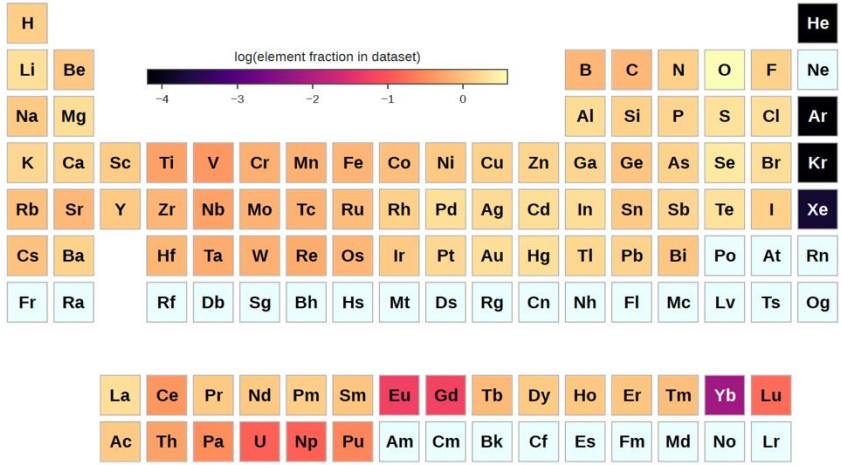

Foundational GRACE

- **True Universality**: The elemental composition of the underlying training set spans most of the periodic table, covering 89 chemical elements, with a focus on inorganic bulk materials.
- **Foundation**: OMAT24 dataset includes more than 110 million structures; OAM models are composed of the OMAT24 dataset, fine-tuned with the subsampled Alexandria (sAlex) and MPTraj (Materials Project) datasets.

materials design

MedeA MLPs

Collection of pre-trained MLPs ready to use with *MedeA* LAMMPS

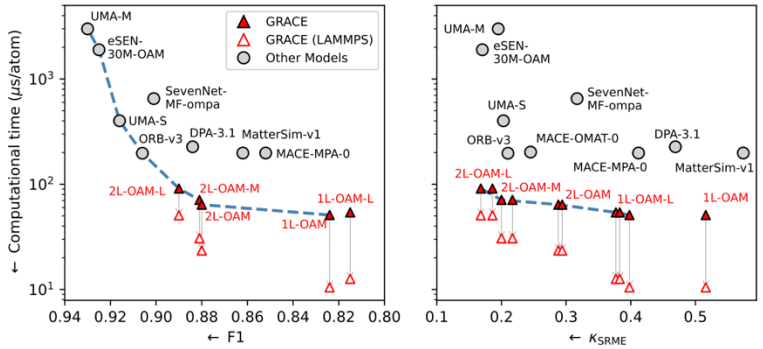

FIG. 1. Model performance for stable structure identification (F1 score in MatBench Discovery benchmark) and thermal conductivity prediction (κ_{SRME}) versus computational time per atom. A higher F1 score and lower κ_{SRME} indicate better performance. The blue dashed line links Pareto optimal models. Computational performance is estimated via ASE (filled symbols) and LAMMPS (open symbols), with GRACE models indicated in red.

Foundational GRACE

- **Validated Accuracy**: Top-ranking in most recent MatBench competitions.
- **Complex property prediction**: Accurately predicts challenging properties, such as thermal conductivity and elastic moduli.
- **Unmatched Efficiency**: Establishes a new ***'Pareto front'***, offering the best available balance between **high accuracy** and **computational speed**.

Y. Lysogorskiy, A. Bochkarev, and R. Drautz, *Graph atomic cluster expansion for foundational machine learning interatomic potentials, arXiv 2508.17936.*

materials design

Zirconium

Phase Transitions, Defects, Elastic and Vibrational Properties

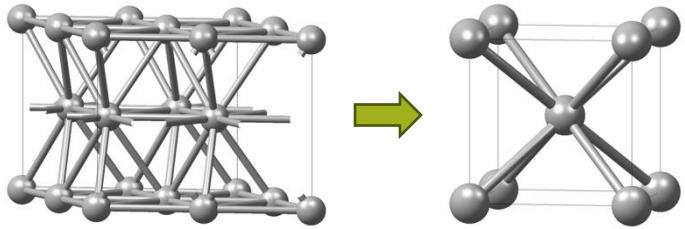

Training Set Creation

Retrieve initial structures from *MedeA* InfoMaticA, the internal structure database

↓

Build strained cells, create randomly perturbed and substituted structures, and perform single-point calculations

↓

Build supercells w/wo self-interstitial atoms and vacancies, surfaces, stacking faults and perform NPT/NVT MD MLFF simulations at 300-1700 K

↓

Training set structures

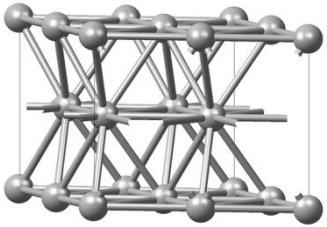

α-phase, hcp

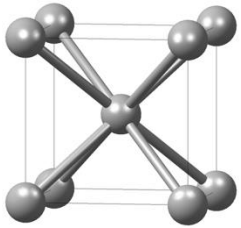

β-phase, bcc

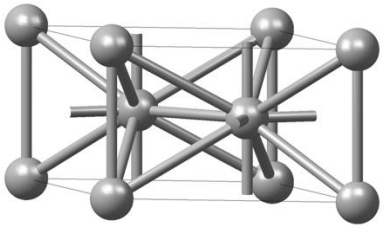

ω-phase, hex

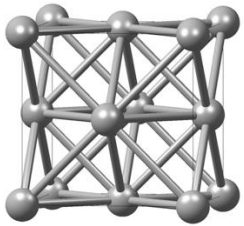

fcc

All calculations use *MedeA* High-Throughput

materials design

Training Set Creation

Retrieve initial structures from *MedeA* InfoMaticA, the internal structure database

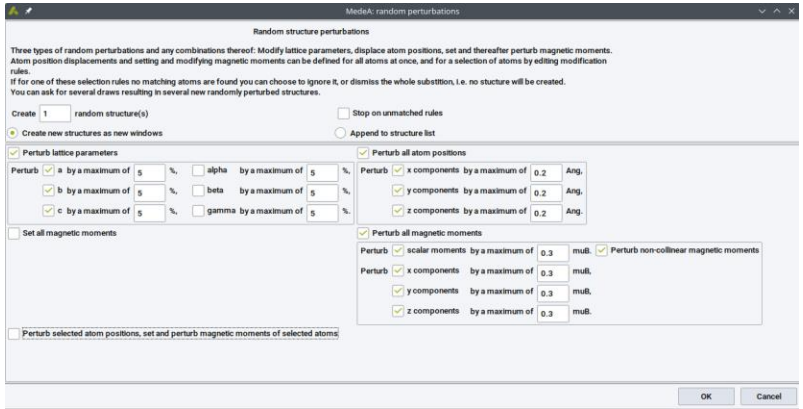

MedeA Random Perturbation/Substitution tools

- Introduce random perturbations of lattice vectors, atomic positions, magnetic moments
- Introduce random changes of atomic species
- Create an arbitrary number of structures
- Results can be appended to structure lists for subsequent high-throughput calculations

Training set structures

All calculations use *MedeA* High-Throughput

materials design

α-Zr: MLP agreement with VASP training data

Structural properties

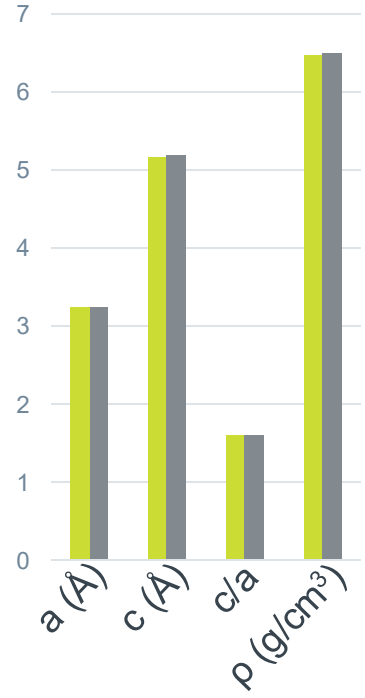

Elastic properties (GPa)

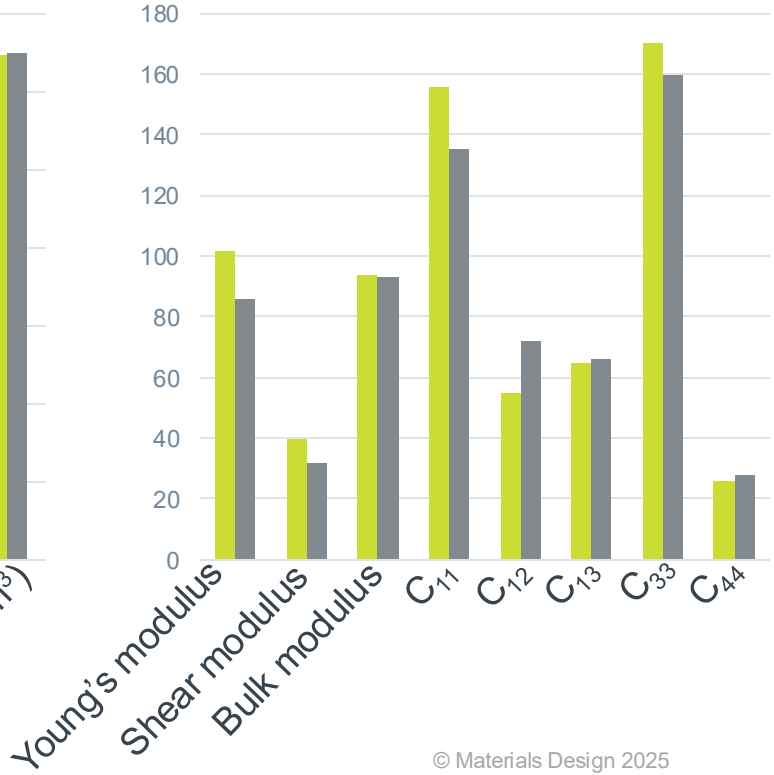

Energetics

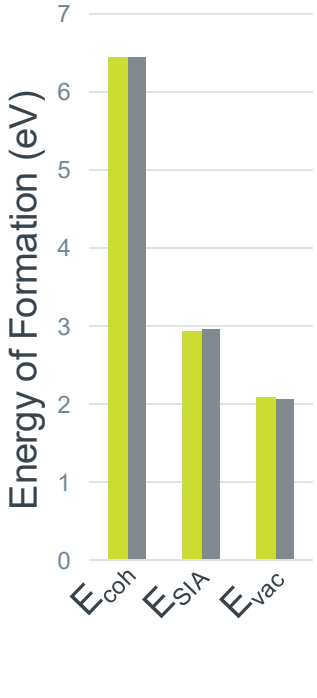

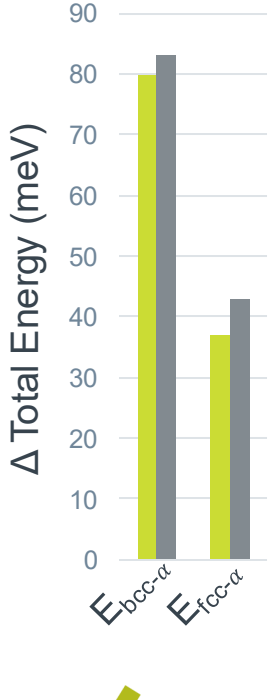

materials design

α-Zr: SNAP Agreement with VASP Training Data

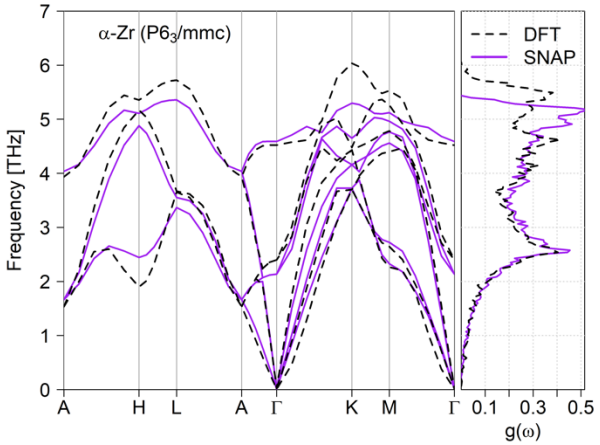

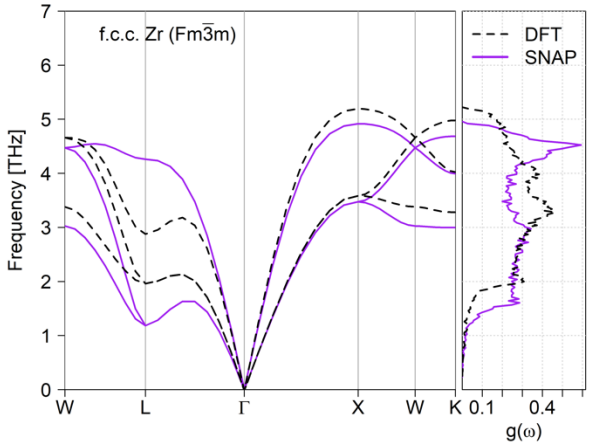

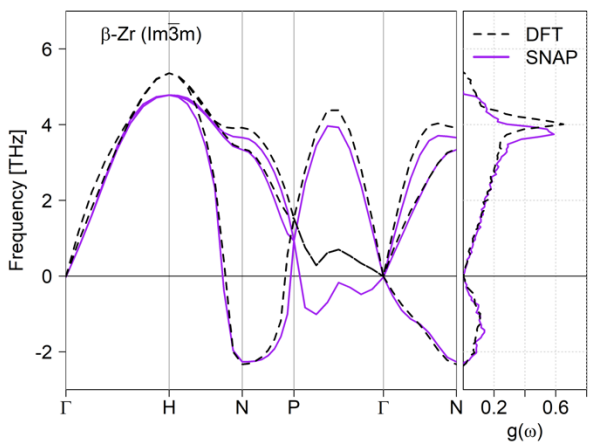

N-point phonon instability
is a precursor of the bcc
→ hcp phase transition

materials design

Zr: α-β Phase Transition

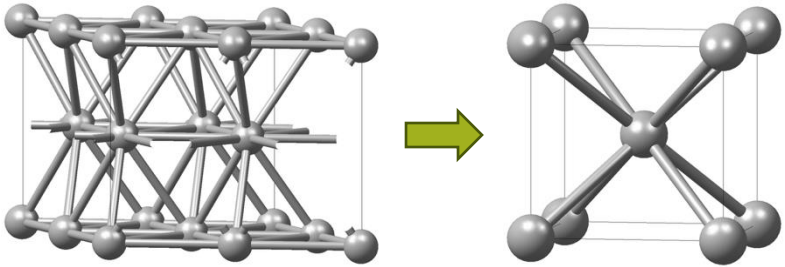

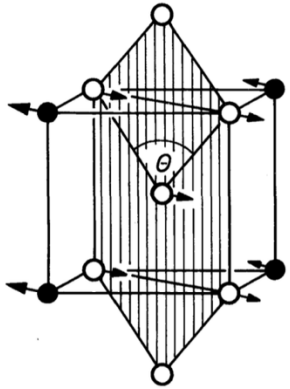

(a) bcc

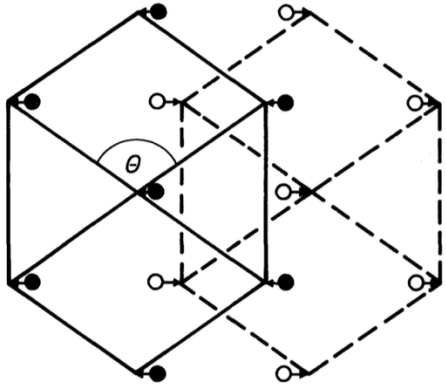

(b)
T_1 N-point
phonon

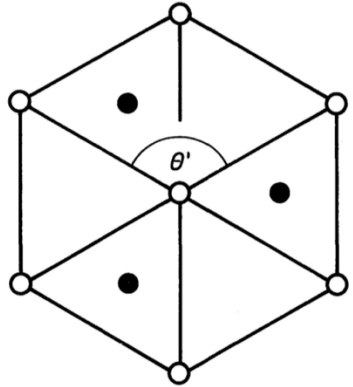

(c)
hcp
angle $\theta \rightarrow \theta'$

Martensitic phase transition at ≈1135 K

- high-T bcc → low-T hcp
- collective motion of atoms
- instability of bcc N-point T_1 phonon

Structural changes

a) involve (110) planes of bcc structure
b) relative shift of neighboring (110) planes
c) change of in-plane angle from Θ=109.47° to Θ'=120°

J. Kübler and V. Eyert, *Electronic structure calculations*, in: *Electronic and Magnetic Properties of Metals and Ceramics*, ed. K. H. J. Buschow (VCH Verlagsgesellschaft, Weinheim 1992), pp. 1-145

materials design

Zr: α-β Phase Transition

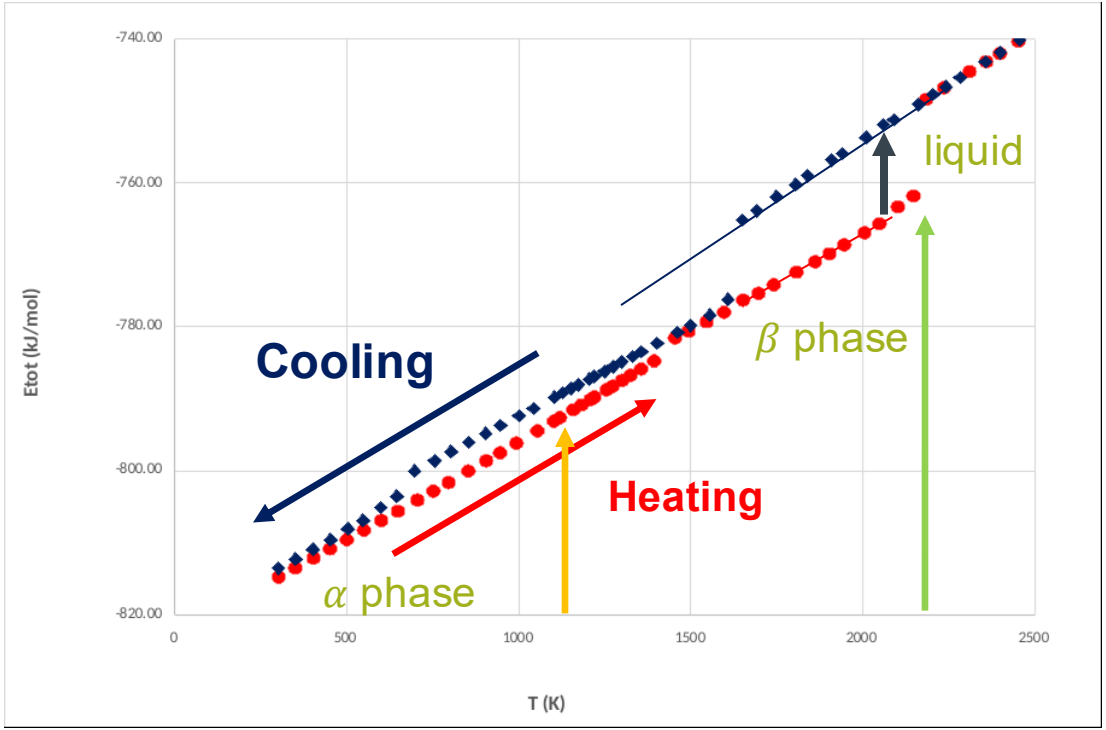

Transition temperatures (exp):
- α-β transition: 1135 K
- melting: 2128 K

Latent heat of α-β transition:
- MLP: ΔH = 2.5 kJ/mol
- Exp.: ΔH = 4.0 kJ/mol

Heat of fusion:
- MLP: ΔH = 13 kJ/mol
- Exp.: ΔH = 14-17 kJ/mol

Specific heat:
- MLP: c_p = 25-31 J/(mol·K)
- Exp.: c_p = 25-39 J/(mol·K)

E. S. Fisher and C. J. Renken, Phys. Rev. **135**, A482 (1964);
M. W. Chase, jr., J. Phys. Chem. Ref. Data **9**, 1 (1998).

MLP capable of capturing multiple coordination environments!

materials design

Zr: α-β Phase Transition

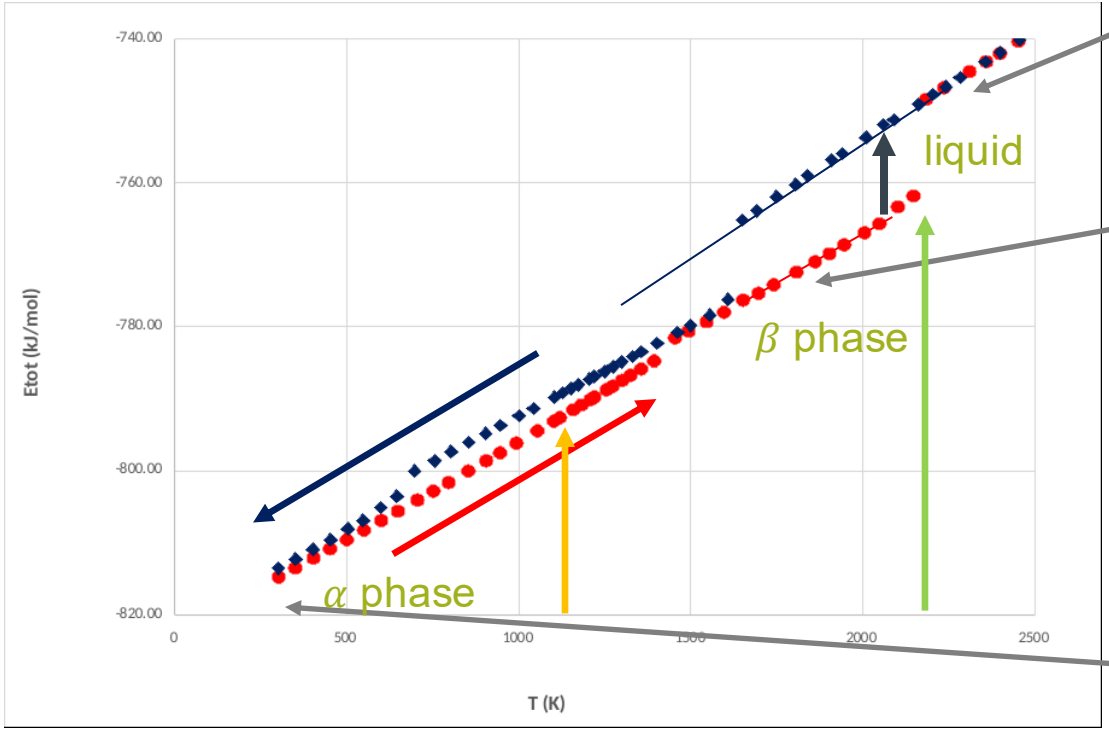

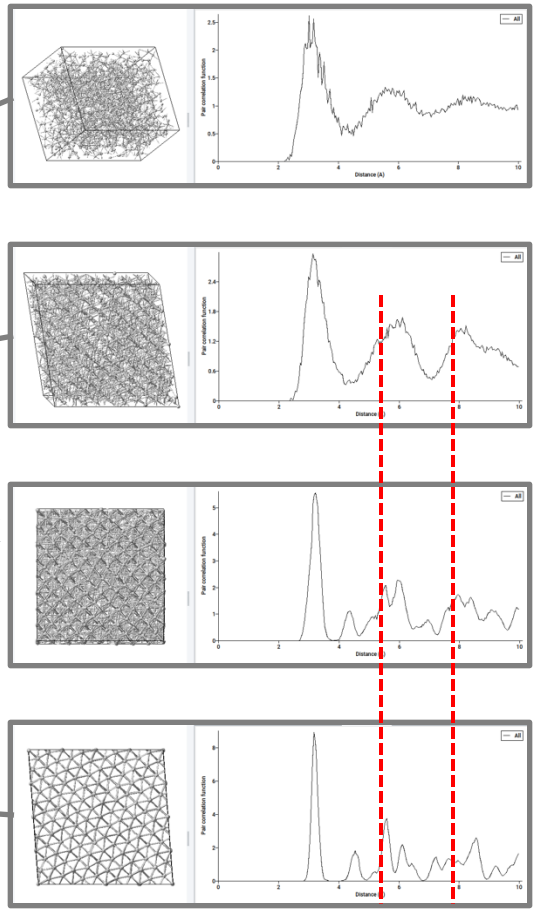

β phase at 300 K

materials design

Zirconium Hydrides

Phase Transitions and Elastic and Vibrational Properties

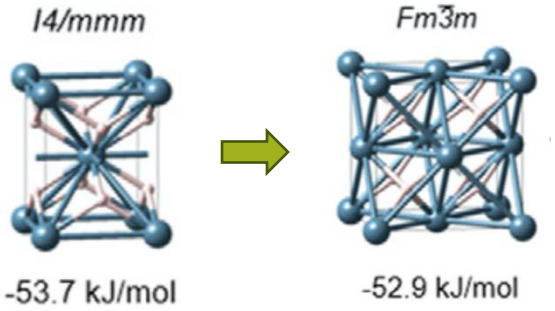

Training Set for ZrH_x

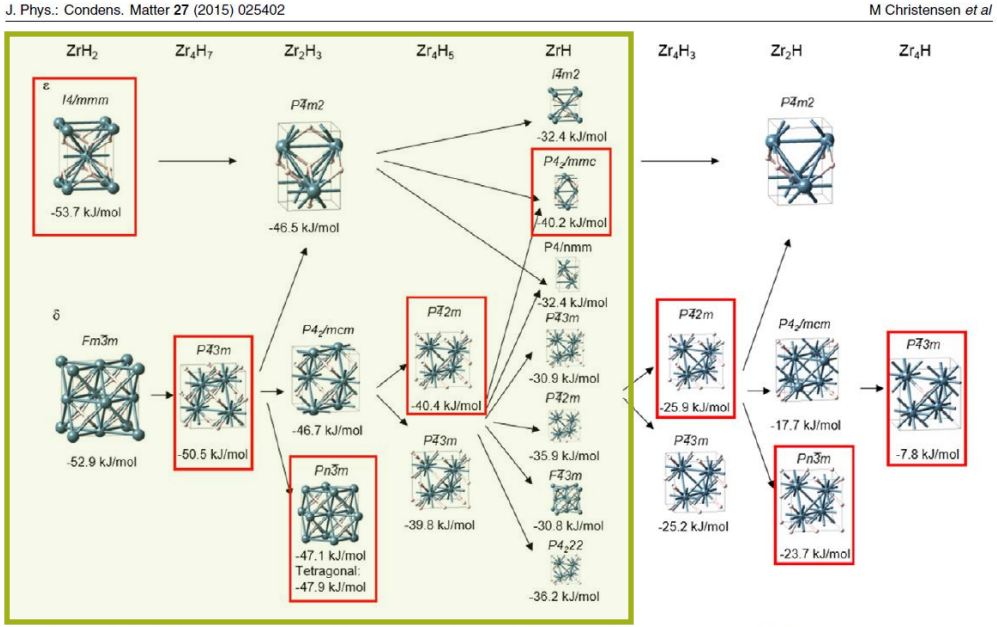

Figure 4. Hydride structures based on ABC stacking of Zr atoms. The most stable structure for each stoichiometry is encircled.

materials design

ZrH_x: Lattice Parameters

γ-ZrH ($P4_2/mmc$)

	Weck	PBE	BMD19.3	SNAP	NNP
a (Å)	4.59	4.59	4.89	4.58	4.58
c (Å)	5.02	4.99	4.49	5.00	5.01

face-centered tetragonal setting

ε-ZrH_2 ($I4/mmm$)

	Weck	PBE	BMD19.3	SNAP	NNP
a (Å)	5.02	4.99	4.85	5.00	5.08
c (Å)	4.42	4.42	4.85	4.42	4.24

face-centered tetragonal setting

Weck *et al.*, Dalton Trans. **44**, 18769 (2015): VASP PBE

ZrH_x: Elastic Coefficients and Moduli

ε-ZrH_2 (I4/mmm)

GPa	Weck	Zhang	PBE	BMD19.3	SNAP	NNP
C_{11}	180	164	176	246	169	217
C_{12}	151	147	146	161	153	175
C_{13}	115	110	104	161	103	129
C_{33}	152	146	159	246	151	159
C_{44}	23	30	62	84	35	65
C_{66}	65	61	82	84	51	64
B	139	132	134	189	132	156
S	28	26	44	64	27	44
Y	77	73	118	172	76	121

materials design

ε-δ-Transition of ZrH_x

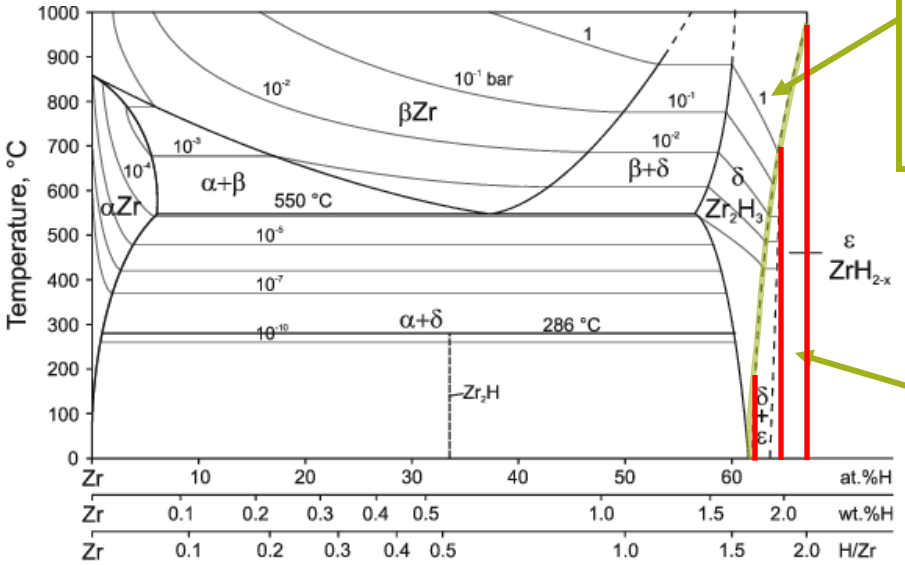

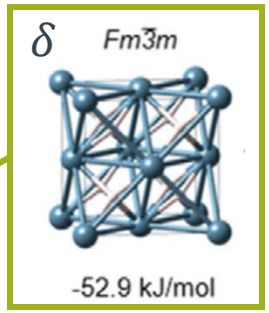

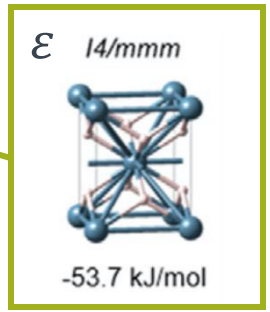

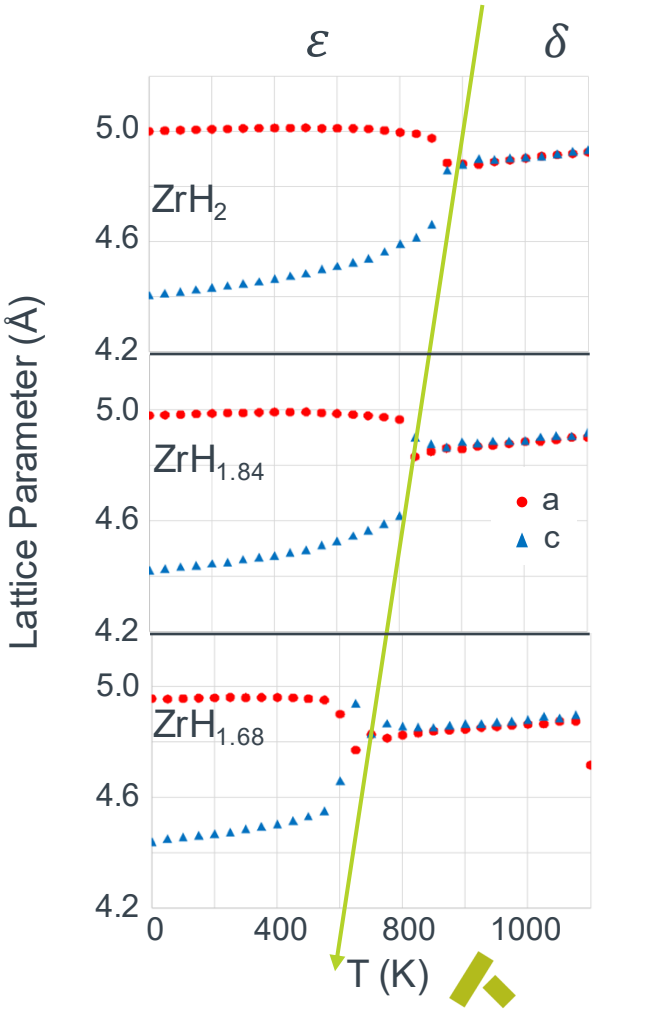

Grosse et al., Oxid Met **70,** 149 (2008)

Sharp decrease of transition temperature with increasing number of H vacancies.

materials design

Zirconium Oxides

Phase Transitions, Defect, and Microstructures

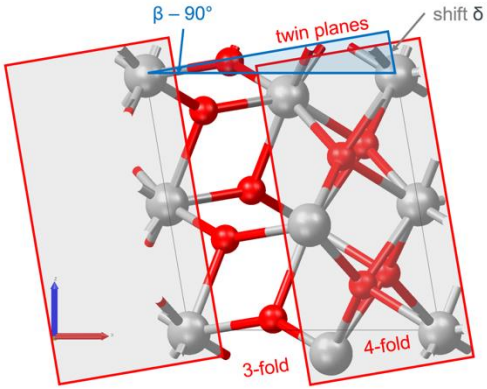

Phase Transitions of ZrO_2

ρ = 6.141 g/cm^3

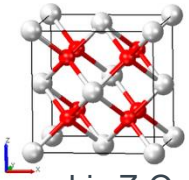

cubic ZrO_2

ρ = 6.099 g/cm^3

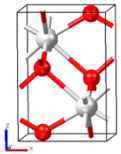

tetragonal ZrO_2

ρ = 5.819 g/cm^3

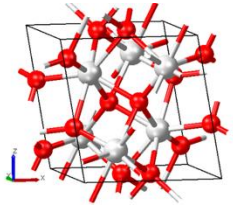

monoclinic ZrO_2

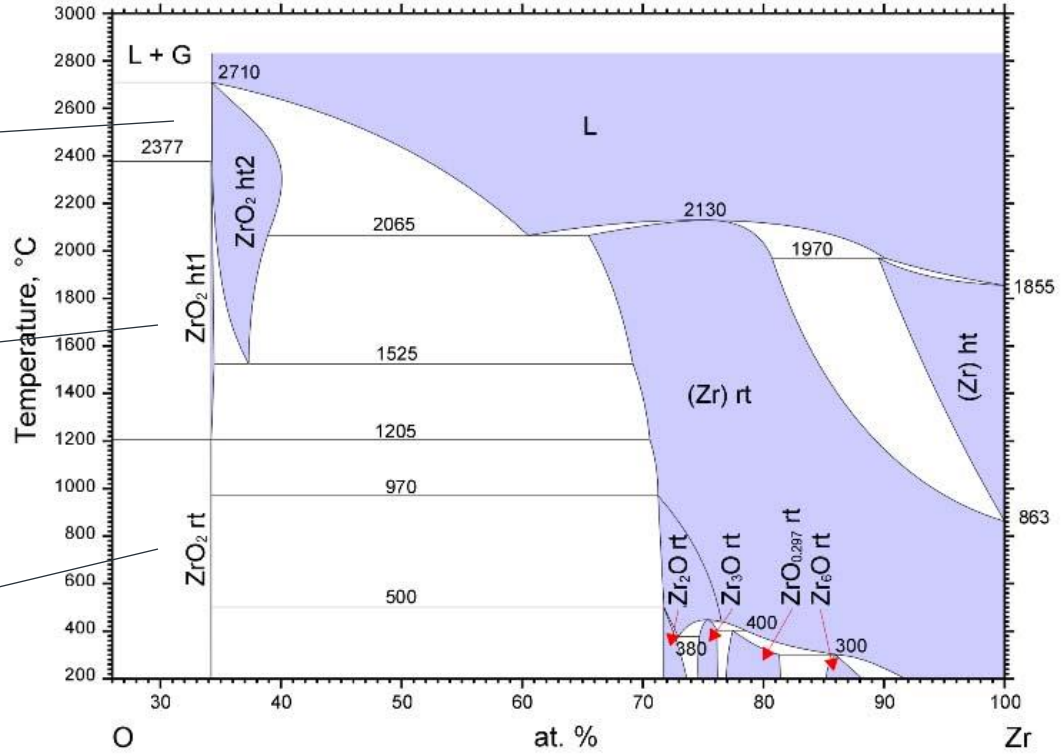

materials design

Training Set for ZrO_x

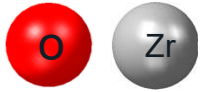

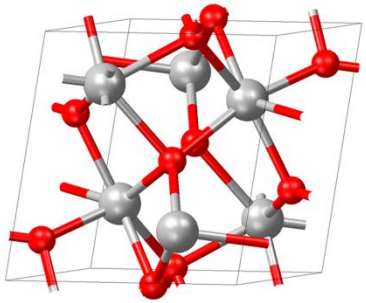

ZrO_2 mon

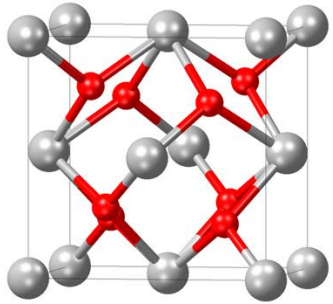

ZrO_2 tet

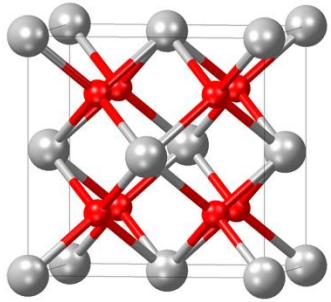

ZrO_2 fcc

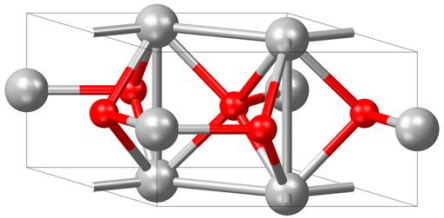

ZrO hex

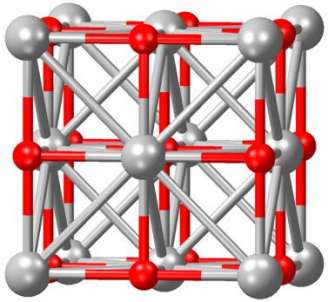

ZrO fcc

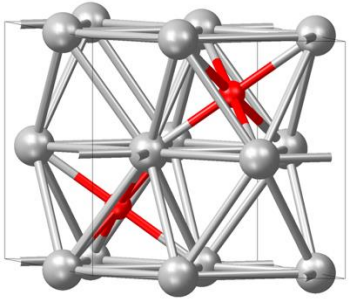

Zr_3O hex

materials design

Phase Transitions of ZrO_2

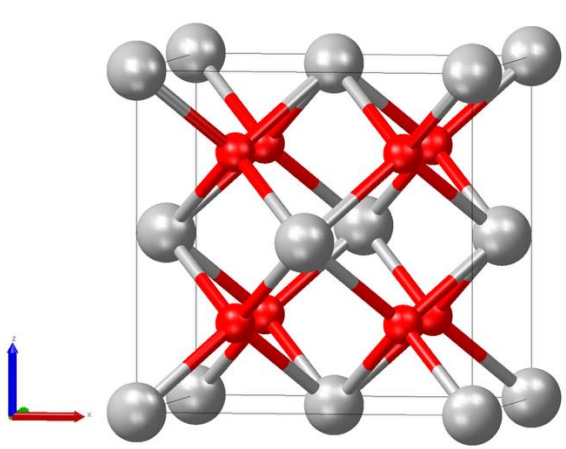

cubic

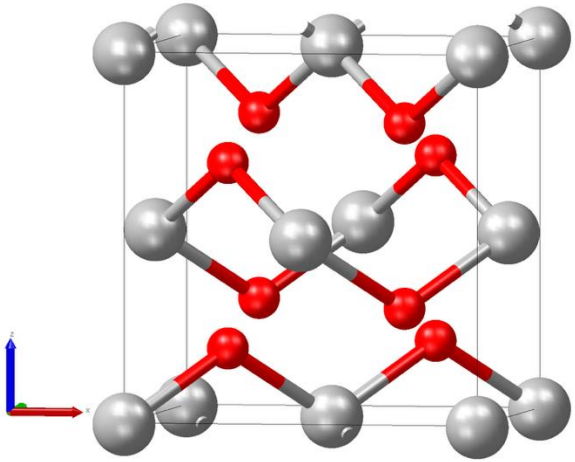

tetragonal

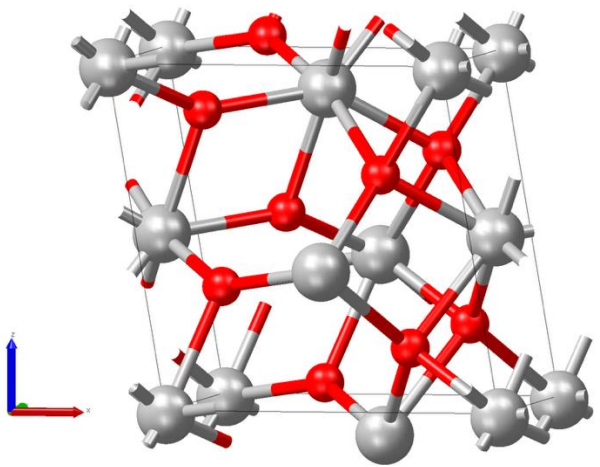

monoclinic

Displacive phase transition at ≈2580 K

- high-T cubic → low-T tetragonal
- instability of fcc X-point phonon

Structural changes

a) Disproportionation of Zr-O bond lengths

Martensitic phase transition at ≈1400 K

- high-T tetragonal → low-T monoclinic

Structural changes

a) Formation of twin Zr planes

b) O coordination: 4-fold → 3-fold

materials design

Phase Transitions of ZrO_2

Martensitic phase transition
- high-T tetragonal → low-T monoclinic

Structural changes
a) formation of twin Zr planes
b) lateral shift δ of neighboring twin planes → induces monoclinic angle β ≠ 90° with $\delta = a_{lat} \times \sin(\beta - 90°)$
c) 4-fold O coordination within twin planes
d) 3-fold O coordination across twin planes

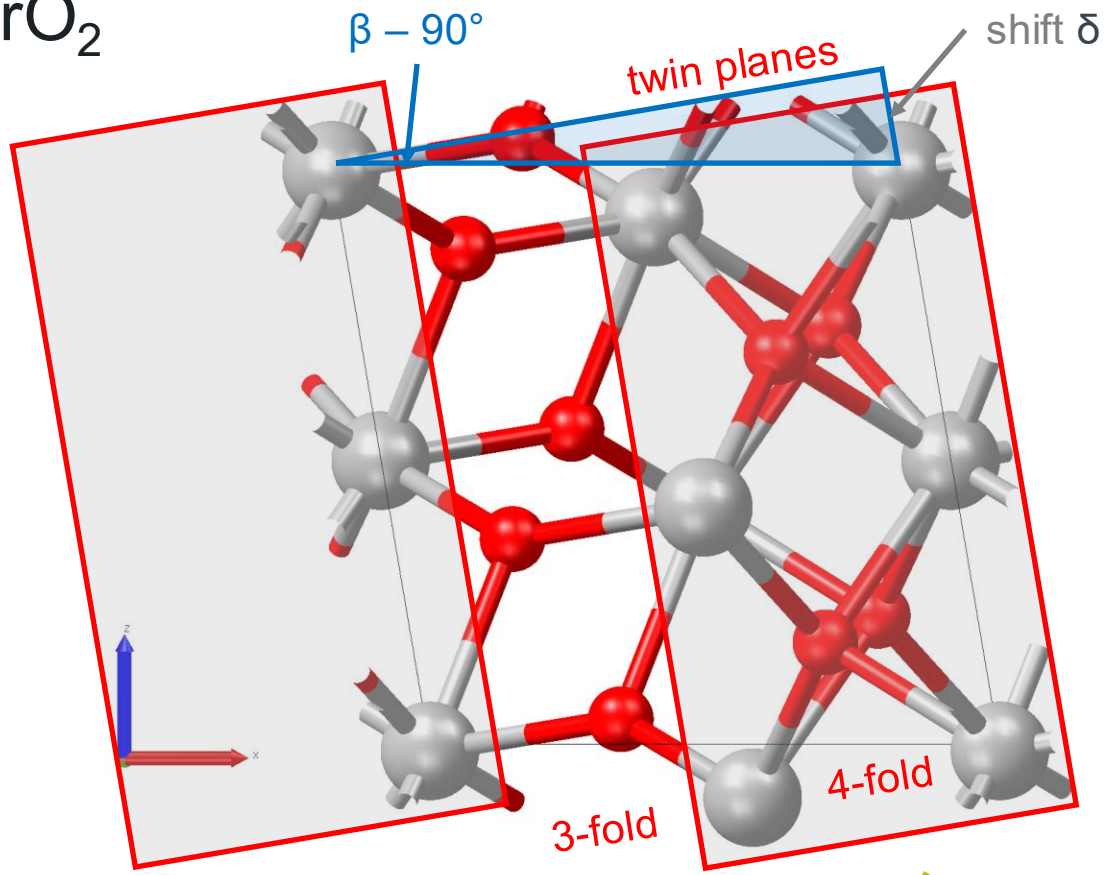

materials design

Phase Transitions of ZrO_2

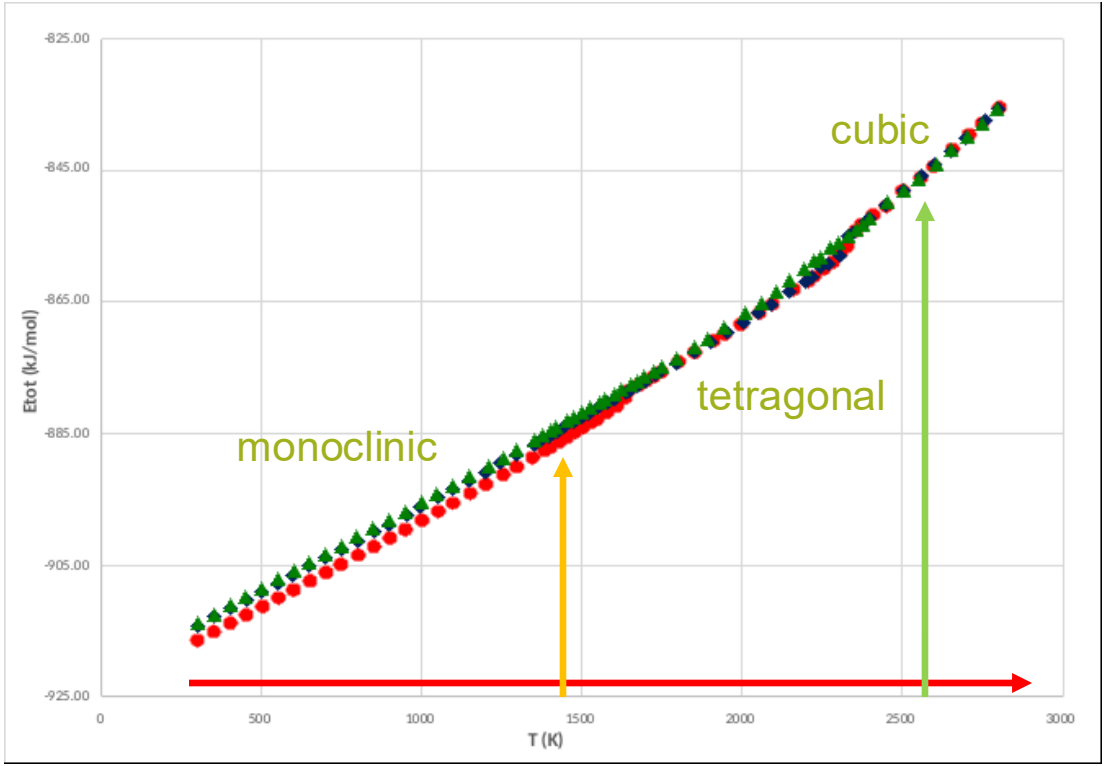

Transition temperatures (exp):

- mon-tet transition:
  - 1430-1474 K (heating)
  - 1305-1264 K (cooling)
- tet-cub: 2584 K

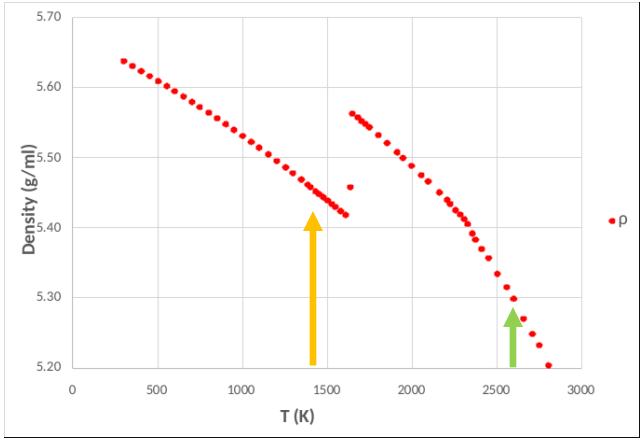

A. Navrotsky et al., J. Am. Ceram. Soc. **88**, 2942 (2005);
C. Wang et al., J. Am. Ceram. Soc. **89**, 3751 (2006);
M. Mamivand et al., Acta Mater. **61**, 5223 (2013)

MLP capable of capturing multiple coordination environments!

materials design

Phase Transitions of ZrO_2

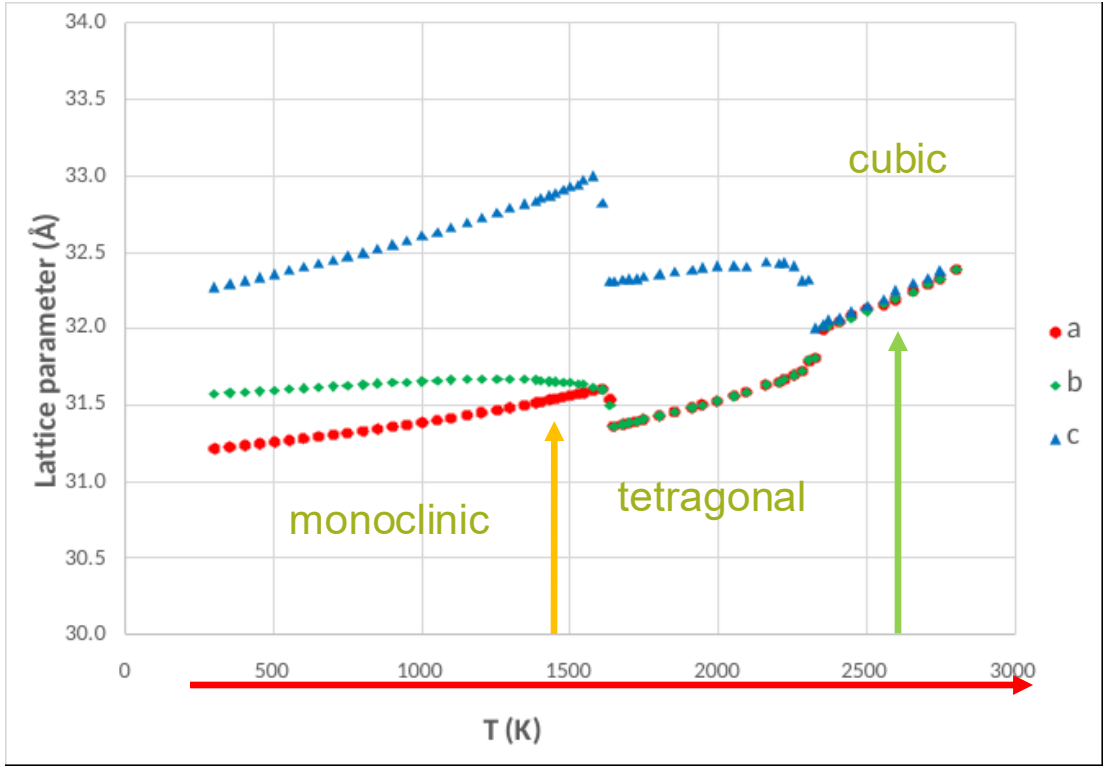

Transition temperatures (exp):

- mon-tet transition:
  - 1430-1474 K (heating)
  - 1305-1264 K (cooling)
- tet-cub: 2584 K

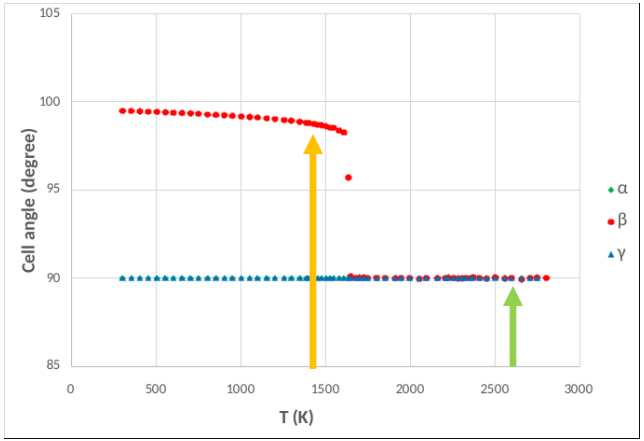

A. Navrotsky et al., J. Am. Ceram. Soc. **88**, 2942 (2005);
C. Wang et al., J. Am. Ceram. Soc. **89**, 3751 (2006);
M. Mamivand et al., Acta Mater. **61**, 5223 (2013)

MLP capable of capturing multiple coordination environments!

materials design

Phase Transition

SiO_2 Polymorphs and Zeolites

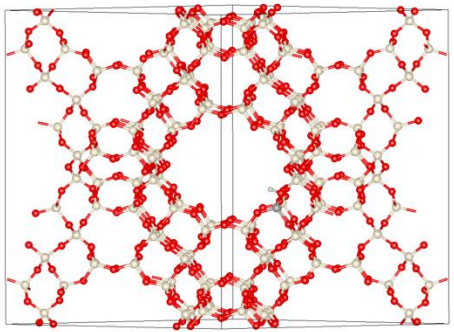

SiO_2 polymorphs and zeolites

- Covalently bonded oxide structures
- Structurally very diverse
- Densely packed (quartz) or with large voids (zeolites)
- Important class of compounds in geochemistry and industry (molecular sieves, catalysts)
- Zeolite unit cells can contain hundreds of atoms

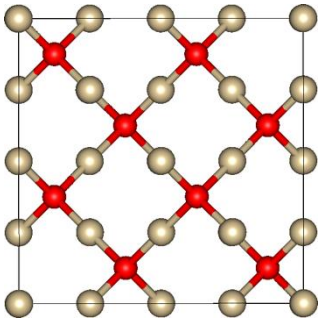

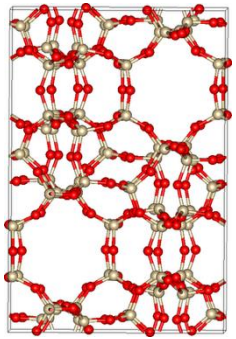

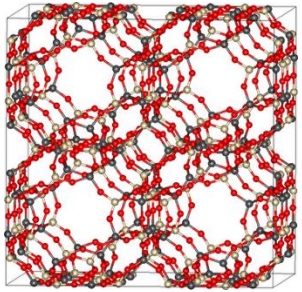

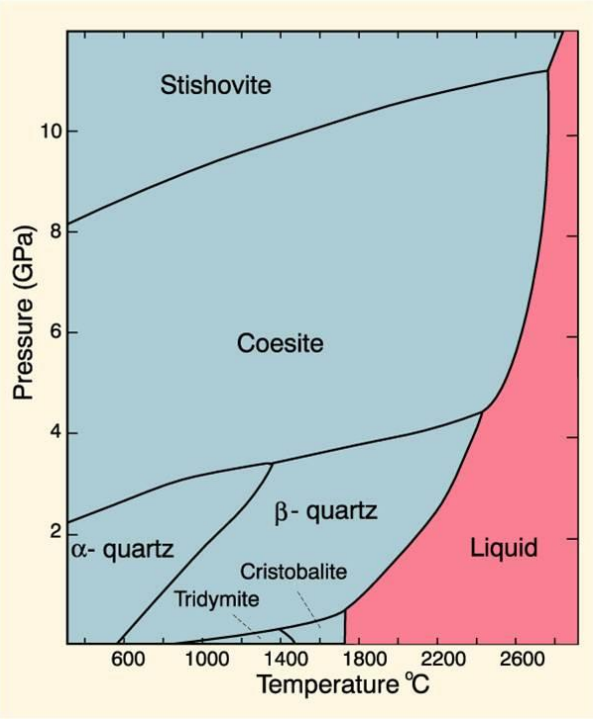

materials design

SiO_2 polymorphs and zeolites – Fitting training set

- DFT GGA-PBE calculations on α-quartz, tridymite and Linde Type A
- Plane-wave cutoff 510 eV, k-spacing 0.178 $Å^{-1}$
- Grimme D3 correction

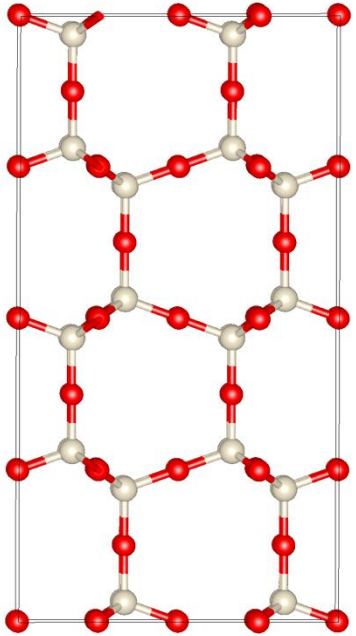

- 206 α-quartz, 341 tridymite and 1184 Linde type A structures
- 90 Linde type A structures with up to three water molecules
- 1821 structures in total
  - Ab initio MD trajectories
  - Systematic distortions of cell parameters and bonds

- MLPs: GRACE-1L and GRACE-2L
- Cutoff 6.0 Å and 10.0 Å,energy weight 1.0, force weight 5.0

materials design

SiO_2 polymorphs and zeolites – Fit quality

		GRACE-1L, 6 Å	GRACE-1L, 10 Å	GRACE-2L
Training set	Energies, RMSE	0.9	1.5	1.0
	Energies, MAE	0.7	1.1	0.8
	Forces, RMSE	19.2	18.4	12.0
	Forces, MAE	12.5	12.3	8.1
Validation set	Energies, RMSE	0.5	1.5	0.6
	Energies, MAE	0.3	0.5	0.3
	Forces, RMSE	39.2	33.9	27.1
	Forces, MAE	16.7	14.7	10.4
Run time	1000 iterations	12 h 51 min	30 h 41 min	24 h 3 min

Energies in meV/atom, forces in meV/Å, run times on Nvidia Geforce RTX 3060

materials design

SiO_2 Polymorphs and Zeolites – MLP Transferability

- LAMMPS minimization, GRACE-1L, cutoff 6 Å

	a(exp.)	b(exp.)	c(exp.)	dev. a [%]	dev. b [%]	dev. c [%]
α-quartz	4.91	4.91	5.4	1.1	0.8	1.0
β-quartz	5	5	5.46	1.3	1.3	2.5
β-cristobalite (high)	7.16	7.16	7.16	173.0	173.0	173.0
α-cristobalite (low)	4.9709	4.9709	6.9278	1.5	1.5	1.4
Faujasite	24.26	24.26	24.26	1.4	1.4	1.4
ZSM-5	20.02	19.9	13.38	1.6	0.6	0.7
Mordenite	18.09	20.52	7.52	1.6	0.5	0.7
Zeolite Rho	14.88	14.88	14.88	1.0	1.0	1.0
Sodalite	8.83	8.83	8.83	2.3	2.3	2.3
Tridymite	18.524	5.003	23.81	1.3	1.1	1.3
Coesite	7.136	12.369	7.174	0.8	1.0	0.9
Chabazite	13.675	13.675	14.767	0.7	0.6	0.8
Linde Type A	11.919	11.919	11.919	0.7	0.7	0.7
Linde Type A (Si/Al = 3)	(11.919)	(11.919)	(11.919)	2.5	2.1	2.0
ZSM-5 (Si/Al = 95)	(20.02)	(19.9)	(13.38)	1.6	0.3	0.3
Linde Type A (Si/Al = 5)	(11.919)	(11.919)	(11.919)	1.6	2.3	1.1

materials design

SiO_2 Polymorphs and Zeolites – MLP Transferability

- LAMMPS minimization, GRACE-1L, cutoff 10 Å

	a(exp.)	b(exp.)	c(exp.)	dev. a [%]	dev. b [%]	dev. c [%]
α-quartz	4.91	4.91	5.4	1.0	0.8	1.1
β-quartz	5	5	5.46	1.0	0.8	3.2
β-cristobalite (high)	7.16	7.16	7.16	126.5	126.5	126.5
α-cristobalite (low)	4.9709	4.9709	6.9278	1.4	1.4	1.4
Faujasite	24.26	24.26	24.26	1.2	1.2	1.2
ZSM-5	20.02	19.9	13.38	1.4	0.2	0.3
Mordenite	18.09	20.52	7.52	1.3	0.2	0.7
Zeolite Rho	14.88	14.88	14.88	0.8	0.8	0.8
Sodalite	8.83	8.83	8.83	2.2	2.2	2.2
Tridymite	18.524	5.003	23.81	1.3	1.3	1.4
Coesite	7.136	12.369	7.174	1.1	1.0	0.9
Chabazite	13.675	13.675	14.767	0.4	0.4	0.5
Linde Type A	11.919	11.919	11.919	0.5	0.5	0.5
Linde Type A (Si/Al = 3)	(11.919)	(11.919)	(11.919)	2.5	2.1	1.8
ZSM-5 (Si/Al = 95)	(20.02)	(19.9)	(13.38)	1.4	0.1	0.1
Linde Type A (Si/Al = 5)	(11.919)	(11.919)	(11.919)	1.5	2.1	0.7

SiO_2 Polymorphs and Zeolites – MLP Transferability

- LAMMPS minimization, GRACE-2L, cutoff 6 A

	a(exp.)	b(exp.)	c(exp.)	dev. a [%]	dev. b [%]	dev. c [%]
α-quartz	4.91	4.91	5.4	1.0	0.8	1.1
β-quartz	5	5	5.46	1.2	0.9	2.8
β-cristobalite (high)	7.16	7.16	7.16	-1.2	-1.2	-1.2
α-cristobalite (low)	4.9709	4.9709	6.9278	1.4	1.4	1.3
Faujasite	24.26	24.26	24.26	1.2	1.2	1.2
ZSM-5	20.02	19.9	13.38	1.5	0.4	0.4
Mordenite	18.09	20.52	7.52	1.6	0.5	0.7
Zeolite Rho	14.88	14.88	14.88	0.8	0.8	0.8
Sodalite	8.83	8.83	8.83	2.2	2.2	2.2
Tridymite	18.524	5.003	23.81	1.3	1.2	1.3
Coesite	7.136	12.369	7.174	1.2	1.0	1.0
Chabazite	13.675	13.675	14.767	0.5	0.5	0.6
Linde Type A	11.919	11.919	11.919	0.6	0.6	0.6
Linde Type A (Si/Al = 3)	(11.919)	(11.919)	(11.919)	2.3	2.1	1.8
ZSM-5 (Si/Al = 95)	(20.02)	(19.9)	(13.38)	1.3	0.2	0.1
Linde Type A (Si/Al = 5)	(11.919)	(11.919)	(11.919)	1.4	2.0	0.7

SiO_2 Polymorphs and Zeolites – Similarity Analysis

- Structures in a fitting data set can be compared using a similarity analysis
- Uses Smooth Overlap of Atomic Positions (SOAP)[a] descriptor
- Reduce training set size to run first principles calculations only on diverse structures (e. g., from a dynamics run with a foundation model)
- Fitting dataset reduced to 128 structures

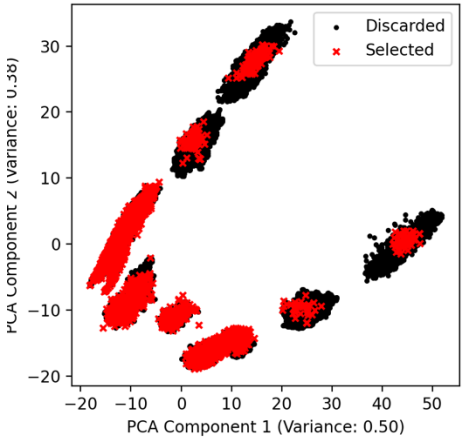

Principal Components Analysis

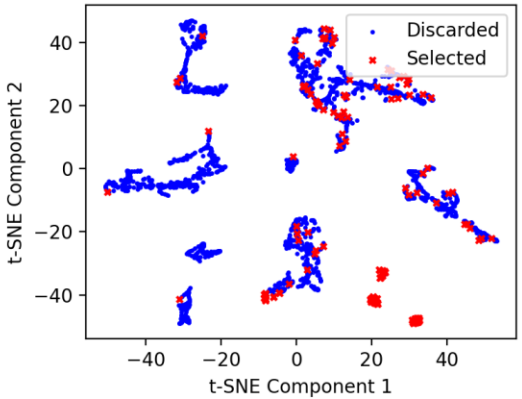

t-distributed Stochastic Neighbor Embedding

[a] Sandip De, Albert P. Bartók, Gábor Csányi, and Michele Ceriotti: Comparing molecules and solids across structural and alchemical space. *Phys. Chem. Chem. Phys.*, **18(20)** (2016), 13754–13769

materials design

SiO_2 polymorphs and zeolites – Similarity Analysis

		GRACE-1L, 6 Å	GRACE-1L, 10 Å	GRACE-2L, 1821 structures	GRACE-2L, 128 structures
Training set	Energies, RMSE	0.9	1.5	1.0	11.1
	Energies, MAE	0.7	1.1	0.8	8.8
	Forces, RMSE	19.2	18.4	12.0	170.6
	Forces, MAE	12.5	12.3	8.1	79.0
Validation set	Energies, RMSE	0.5	1.5	0.6	4.7
	Energies, MAE	0.3	0.5	0.3	3.8
	Forces, RMSE	39.2	33.9	27.1	102.5
	Forces, MAE	16.7	14.7	10.4	68.6
Run time	1000 iterations	12 h 51 min	30 h 41 min	24 h 3 min	6 h 30 min

Energies in meV/atom, forces in meV/Å, run times on Nvidia Geforce RTX 3060

SiO_2 Polymorphs and Zeolites – Similarity Analysis

	GRACE-2L, 1821 structures			GRACE-2L, 128 structures		
	dev. a [%]	dev. b [%]	dev. c [%]	dev. a [%]	dev. b [%]	dev. c [%]
α-quartz	1.0	0.8	1.1	0.7	0.5	1.1
β-quartz	1.2	0.9	2.8	3.2	3.1	-0.4
β-cristobalite (high)	-1.2	-1.2	-1.2	8.6	8.6	8.6
α-cristobalite (low)	1.4	1.4	1.3	1.8	1.8	1.5
Faujasite	1.2	1.2	1.2	0.4	0.4	0.4
ZSM-5	1.5	0.4	0.4	-0.1	-1.9	-0.9
Mordenite	1.6	0.5	0.7	0.8	0.0	0.0
Zeolite Rho	0.8	0.8	0.8	-0.1	-0.1	-0.1
Sodalite	2.2	2.2	2.2	1.3	1.3	1.3
Tridymite	1.3	1.2	1.3	1.1	1.1	1.5
Coesite	1.2	1.0	1.0	1.9	-53.6	-23.8
Chabazite	0.5	0.5	0.6	-0.3	-0.3	-0.1
Linde Type A	0.6	0.6	0.6	-0.2	-0.2	-0.2
Linde Type A (Si/Al = 3)	2.3	2.1	1.8	0.0	-0.2	-0.2
ZSM-5 (Si/Al = 95)	1.3	0.2	0.1	0.6	-0.4	-0.8
Linde Type A (Si/Al = 5)	1.4	2.0	0.7	-0.6	-0.9	-1.7

Co Nanoclusters

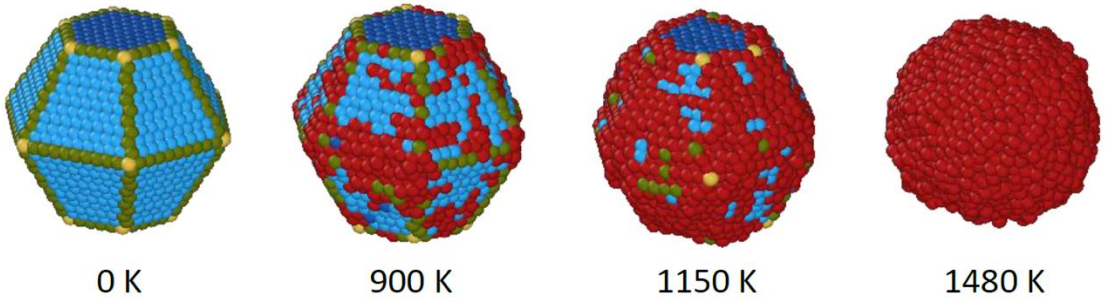

Dynamics of Co Nanoparticles: A Machine Learning Approach[1]

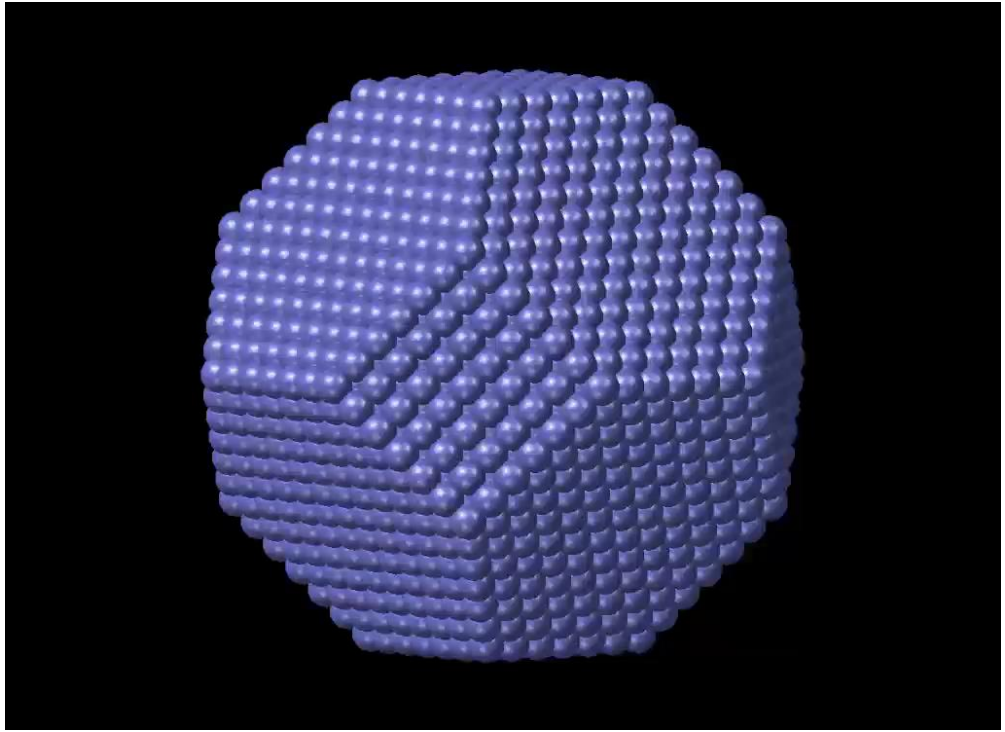

Molecular dynamics simulation of a truncated octahedral fcc Co nanoparticle using a machine-learning potential [1].

Heating from 1 K to 2000 K in 30 ps

[1] M. Bideault, J. Creuze, R. Asahi, and E. Wimmer, Polyvalent machine-learned potential for cobalt: From bulk to nanoparticles, Phys. Rev. Materials **8**, 123803 (2024)

materials design

Dynamics of Co Nanoparticles: A Machine Learning Approach[1]

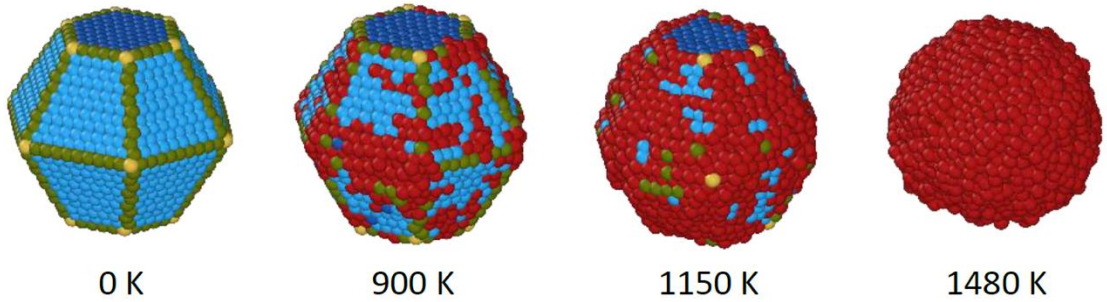

Classification of atoms using machine learning with a bispectrum descriptor

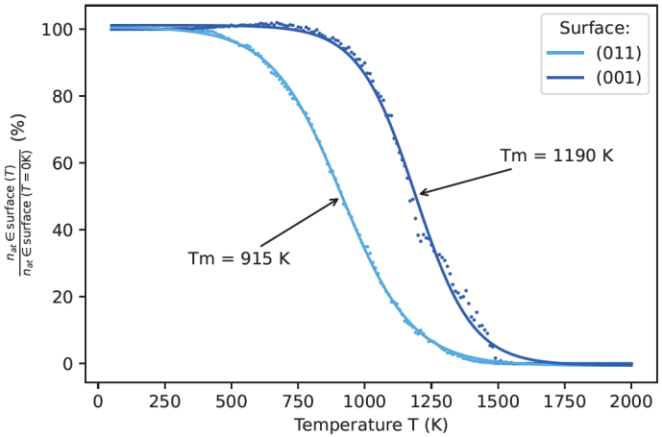

- The (011) facets of an hcp-type nanoparticle melt at 915 K
- The (001) facets are more stable, melting at 1190 K
- The entire nanoparticle melts at 1480 K
- The computed melting point of bulk Co is 1695 ± 15 K; experiments: 1768 K and 1770 K

[1] M. Bideault, J. Creuze, R. Asahi, and E. Wimmer, Polyvalent machine-learned potential for cobalt: From bulk to nanoparticles, Phys. Rev. Materials **8**, 123803 (2024)

materials design

MedeA MLP/MLPG

VASP accuracy with LAMMPS speed at your fingertips all within *MedeA*

- Machine-Learned-Potentials (MLPs) offer a combination of extended length and time scales with unprecedented ease in generation and high fidelity with respect to DFT to describe so far inaccessible physical phenomena.
- The *MedeA* MLP Generator (MLPG) offers a fully integrated workflow from training-set generation (using *MedeA* HT) and MLP generation to MLP application using *MedeA* LAMMPS.
- Foundational GRACE potentials are ready to use with *MedeA* LAMMPS.

Question and Answer Session

Dr. Volker Eyert

Materials Design

Dr. Jörg-Rüdiger Hill

Materials Design

Questions about Materials Design Webinars

Katherine Hollingsworth

khollingsworth@materialsdesign.com

materials design

info@materialsdesign.com

www.materialsdesign.com

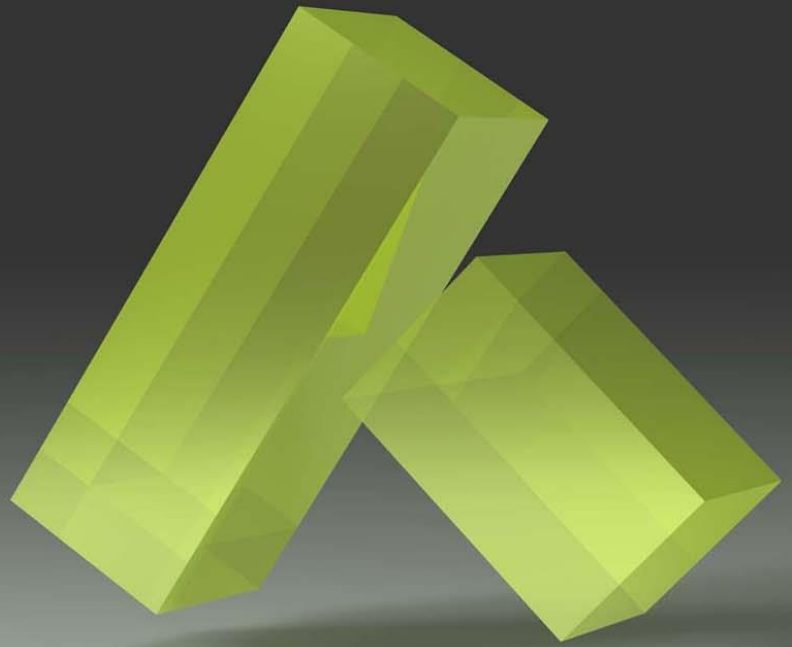

MedeA

Innovation by Simulation

Additional Material

JMR Focus Issue on MLPs

- J. Mater. Res. **38**(24), 2023
- Guest editors: Volker Eyert, Jonathan Wormald, William A. Curtin, Erich Wimmer
- Introductory article by guest editors
- Nine additional publications
  - Combination of methodology and applications
  - Two invited feature articles: Ralf Drautz *et al.*, Aidan Thompson, Mitchell Wood *et al.*
  - Seven invited articles: Gus Hart *et al.*, Ryoji Asahi *et al.*, Alexander Shapeev *et al.*, Michele Ceriotti, William Curtin *et al.*, Jörg-Rüdiger Hill and Wolfgang Mannstadt

materials design

Introductory Paper

- Historical outline from classical forcefields to machine-learned potentials
- Key features of MLPs
- Approaches to generate MLPs
- MLFF, active learning, Δ-learning
- Basic concepts (descriptors, regressors)
- Applications of MLPs (literature survey)
- Overview of the Focus Issue
- Perspectives

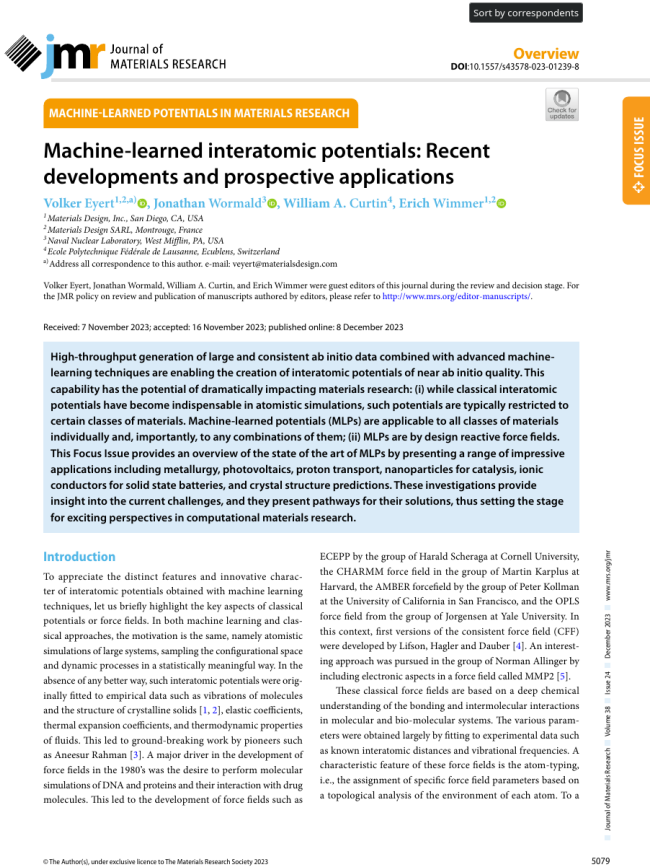

Sort by correspondents

jmr Journal of MATERIALS RESEARCH

Overview

DOI:10.1557/s43578-023-01239-8

MACHINE-LEARNED POTENTIALS IN MATERIALS RESEARCH

FOCUS ISSUE

Machine-learned interatomic potentials: Recent developments and prospective applications

Volker Eyert[1,2,a], Jonathan Wormald[3], William A. Curtin[4], Erich Wimmer[1,2]

[1] Materials Design, Inc., San Diego, CA, USA
[2] Materials Design SARL, Montrouge, France
[3] Naval Nuclear Laboratory, West Mifflin, PA, USA
[4] Ecole Polytechnique Fédérale de Lausanne, Ecublens, Switzerland
[a] Address all correspondence to this author. e-mail: veyert@materialsdesign.com

Volker Eyert, Jonathan Wormald, William A. Curtin, and Erich Wimmer were guest editors of this journal during the review and decision stage. For the JMR policy on review and publication of manuscripts authored by editors, please refer to http://www.mrs.org/editor-manuscripts/.

Received: 7 November 2023; accepted: 16 November 2023; published online: 8 December 2023

High-throughput generation of large and consistent ab initio data combined with advanced machine-learning techniques are enabling the creation of interatomic potentials of near ab initio quality. This capability has the potential of dramatically impacting materials research: (i) while classical interatomic potentials have become indispensable in atomistic simulations, such potentials are typically restricted to certain classes of materials. Machine-learned potentials (MLPs) are applicable to all classes of materials individually and, importantly, to any combinations of them; (ii) MLPs are by design reactive force fields. This Focus Issue provides an overview of the state of the art of MLPs by presenting a range of impressive applications including metallurgy, photovoltaics, proton transport, nanoparticles for catalysis, ionic conductors for solid state batteries, and crystal structure predictions. These investigations provide insight into the current challenges, and they present pathways for their solutions, thus setting the stage for exciting perspectives in computational materials research.

Introduction

To appreciate the distinct features and innovative character of interatomic potentials obtained with machine learning techniques, let us briefly highlight the key aspects of classical potentials or force fields. In both machine learning and classical approaches, the motivation is the same, namely atomistic simulations of large systems, sampling the configurational space and dynamic processes in a statistically meaningful way. In the absence of any better way, such interatomic potentials were originally fitted to empirical data such as vibrations of molecules and the structure of crystalline solids [1, 2], elastic coefficients, thermal expansion coefficients, and thermodynamic properties of fluids. This led to ground-breaking work by pioneers such as Aneesur Rahman [3]. A major driver in the development of force fields in the 1980's was the desire to perform molecular simulations of DNA and proteins and their interaction with drug molecules. This led to the development of force fields such as ECEPP by the group of Harald Scheraga at Cornell University, the CHARMM force field in the group of Martin Karplus at Harvard, the AMBER forcefield by the group of Peter Kollman at the University of California in San Francisco, and the OPLS force field from the group of Jorgensen at Yale University. In this context, first versions of the consistent force field (CFF) were developed by Lifson, Hagler and Dauber [4]. An interesting approach was pursued in the group of Norman Allinger by including electronic aspects in a force field called MMP2 [5].

These classical force fields are based on a deep chemical understanding of the bonding and intermolecular interactions in molecular and bio-molecular systems. The various parameters were obtained largely by fitting to experimental data such as known interatomic distances and vibrational frequencies. A characteristic feature of these force fields is the atom-typing, i.e., the assignment of specific force field parameters based on a topological analysis of the environment of each atom. To a

J. Mater. Res. **38**, 5079 (2023)

materials design

Datasheets, Tutorials, Documentation

materials design

MedeA MLP

Efficient and Flexible Machine Learning Potential Support

At-a-Glance

MedeA® MLP (*Machine Learning Potential*) provides full *MedeA* support for LAMMPS based machine learning potential simulations, including the simulation of mechanical, vibrational, and transport properties combined with comprehensive *MedeA* based analysis of simulation results.

MedeA MLP includes a library of published machine learning potentials derived from the Spectral Neighbor Analysis Potential (SNAP)[2] formalism supported by LAMMPS.

MedeA LAMMPS based simulations using *MedeA MLP* typically show excellent agreement with first-principles methods for systems that are well represented by the training set employed in creating the machine learning potential.

Key Benefits

Productivity

- Extends *ab initio* simulation results to larger length and time scales through substantially reduced energy and force calculation times
- Efficient use of published machine learning potentials
- Automates the handling of files and data for efficient simulation

Access

- Supports the SNAP machine learning potential form
- Allows access to all *MedeA LAMMPS* simulation properties with machine learning potential accuracy
- Can be employed with the *Machine Learning Potential Generator* (*MedeA MLPG*) to access newly derived machine learning potentials
- Handles diverse atomic geometries including making and breaking of bonds

Machine learning methods allow rich first-principles datasets to be mined and employed in interpolation and inference. Such techniques are having a dramatic effect in many areas of science. In materials science, they allow researchers to obtain the accuracy and freedom from bias of *ab initio* methods at reasonable computational cost for substantial simulation times and system sizes.

'All science depends on past work. Machine Learning depends more than other science on previous work: it needs examples.'

Michael Levitt, Nobel Laureate.

Machine learning based methods for energy and force calculation have been used for a number of years. For example, Blank et al. in 1995 employed a neural net based methodology to probe the energetics of CO on the Ni(111) surface[3]. In recent years it has become increasingly clear that such approaches, employing novel descriptors and advanced machine learning techniques, can yield exceptionally accurate reproduction of quantum mechanical training data at substantially reduced computational cost[4].

MedeA MLP provides easy to use and efficient access to such methods. By making such machine learning potentials accessible for use with *MedeA LAMMPS*, *MedeA MLP* extends the range of *ab initio* methods to much larger length and time scales, while relying on first-principles results for

[1] MedeA and Materials Design are registered trademarks of Materials Design, Inc.
[2] A. P. Thompson, L. P. Swiler, C. R. Trott, S. M. Foiles, and G. J. Tucker, *Spectral neighbor analysis method for automated generation of quantum-accurate interatomic potentials*, J. Comp. Phys. **285**, 316 (2015)
[3] T. B. Blank, S. D. Brown, A. W. Calhoun, D. J. Doren, *Neural network models of potential energy surfaces*, J. Chem. Phys., **103**, 4129 (1995)
[4] J. Behler, and M. Parrinello, *Generalized neural-network representation of high-dimensional potential energy surfaces*, Phys. Rev. Lett. **98**, 146401 (2007)

Key Features

- Library of published machine learning potentials
- Full support for the SNAP description
- Enables LAMMPS MLP simulations in the *MedeA Environment*

Required Modules

MedeA Environment
MedeA LAMMPS

lated Modules

deA MT
deA Phonon
deA Diffusion
eA Surface Tension
eA Thermal Conductivity

Out More

re about Machine Learning by watching
ar: https://www.materialsdesign.com/
ecorded/Machine-Learning-Quantum%
mistry-Catalysts

Deng, R. Tran, H. Tang, I. H. Chu, S. P. Ong, *e field for molybdenum by machine learning data*, Phys. Rev. Mater. **1**, 043603 (2017)
Hu, C. Chen, Z. Deng, J. Luo, S. P. *-accurate spectral neighbor analysis potential Ni-Mo binary alloys and fcc metals*, Phys. 04 (2018)
A. Cusentino, B. D. Wirth, A. P. Thompson, *rial models for atomistic simulation*, Phys. 5 (2019)
X. Li, Z. Deng, Y. Chen, J. Behler, S. P. *and cost assessment of machine learning potentials*, J. Phys. Chem. A, **124**, 731
A. Wood, and A. P. Thompson, *Explicit ion of the Spectral Neighbor Analysis ally Complex Systems*, J. Phys. Chem.
H. Zheng, Y. Zuo, S. P. Ong, *Comechanisms in the NbMoTaW multi-*, npj Comput. Mater. **6**, 70 (2020)

materials design

materials design

MedeA MLPG

Efficient Flexible Machine Learning Potential Generator

At-a-Glance

The *MedeA*® *MLPG* (Machine Learning Potential Generator) enables users to create their own machine learning potentials (or force-fields) from training-set data previously generated by quantum mechanical calculations. The resulting potentials allow users to perform simulations of systems substantially larger in size and for much larger simulation times than can be typically accessed using quantum mechanical methods while at the same time reflecting the high accuracy and validity of the latter.

In addition to managing selection of training and validation data, the *MedeA MLPG* allows you to generate machine learning potentials, using the Spectral Neighbor Analysis Potential (SNAP)[2] formalisms. The potentials created are ready for subsequent use with *MedeA MLP*. Combined with the *MedeA* Flowchart Interface as well as VASP and LAMMPS, the *MedeA MLPG* thus provides efficient access to machine learning based simulation techniques.

Key Benefits

Productivity

- Automates the creation of machine learning potentials using the SNAP formalism
- Extends *ab initio* precision to larger length and time scales
- Manages training set data
- Full Ziegler-Biersack-Littmark (ZBL) potential support

Accuracy

- Yields machine learning descriptions based on the SNAP methods
- Provides access to all calculation details and information
- Provides machine learning potentials for use with all *MedeA LAMMPS* property calculation types

Machine learning potentials employ efficient descriptors of atomic environments combined with machine learning based correlative methods to describe the energetic behavior of atomic and molecular systems. The *MedeA MLPG* allows users to generate machine learning potentials by accurately reproducing supplied target first-principles data for a training set of structures.

Figure 1: The MedeA Machine Learning Potential Generator (MLPG) is integrated within the MedeA environment allowing straightforward use of first-principles information from VASP in the creation of MLPs.

The *MedeA MLPG* manages training-set data derived from first-principles calculations as the target to be reproduced by the MLP (machine learning potential). Configuration dependent energies, forces, and stresses can be considered in the fitting process. Using the SNAP approach the *MedeA MLPG* creates a machine learning potential by minimizing the deviations from the target energies, forces, and stresses calculated by quantum mechanical methods. While this process is guided by meaningful default parameters, the full flexibility of the underlying methods can be accessed by advanced settings. The *MedeA MLPG* has been developed as part of active research and development projects and is thoroughly validated.

[1] MedeA and Materials Design are registered trademarks of Materials Design, Inc.
[2] A. P. Thompson, L. P. Swiler, C. R. Trott, S. M. Foiles, and G. J. Tucker, *Spectral neighbor analysis method for automated generation of quantum-accurate interatomic potentials*, J. Comp. Phys. **285**, 316 (2015)

Technical Features

User Interface

- Selection of training and validation data
- Specification of terms for optimization
- Report and plot creation for analysis

Supported Target Data

Energies
Forces
Stress tensors

ey Features

Uses VASP derived DFT results
teractive selection and control
utomated results analysis
fficient handling of optimization

ired Modules

Environment
MLP
VASP
LAMMPS

Modules

nnon
sion
ce Tension
mal Conductivity

lore

t Machine Learning by watching
ttps://www.materialsdesign.com/
/Machine-Learning-Quantum%
Catalysts

materials design

materials design

Related *MedeA* Webinars

Ab Initio for Millions - the Power of Machine-learned Potentials:
https://www.materialsdesign.com/webinars/recorded/Ab-Initio-for-MLPG

***MedeA* Training: *MedeA* Machine Learning Potential Generator (MLPG):**
https://www.materialsdesign.com/webinars/recorded/UGM-2021-Training-MLPG

VASP, Machine Learning, and Multi-Scale Physics: Defining the State of the Art in Materials Modeling:
https://www.materialsdesign.com/webinars/recorded/MedeA-VASP-Machine-Learning

Training: Generating and Applying Machine-Learned Potentials with *MedeA*:
https://www.materialsdesign.com/webinars/recorded/UGMtraining-Generating-and-Applying-Machine-Learned-Potentials-with-MedeA

On-the-fly Machine Learning Forcefields with *MedeA* VASP:
https://www.materialsdesign.com/webinars/recorded/MedeA-Training-On-the-Fly-Machine-Learning-Forcefields-with-MedeA-VASP

materials design

Related *MedeA* Tutorials

An Introduction to *MedeA* MLP:

Learn how to run LAMMPS simulations with Machine Learning Potential

An Introduction to *MedeA* MLPG:

Learn how to generate machine-learned potentials within *MedeA*

Generate a Ti Neural Network Machine-Learned Potential:

Learn how to generate a neural network potential using *MedeA* MLPG

Applying Delta-Learning to TiO_2 Machine-Learned Potentials:

Learn how to use Δ-learning to upgrade a machine-learned potential for TiO_2 from a lower first-principles level to a higher one

materials design

Highlighted *MedeA* Modules

***MedeA* VASP:** Comprehensive access to the VASP Code via a graphical user interface (GUI) to set up, run and analyze multi-step VASP calculations

***MedeA* MLPG:** Fully integrated workflow from training-set generation (using *MedeA* HT) and MLP generation to MLP application using *MedeA* LAMMPS

***MedeA* HT:** Generation of large and consistent sets of computed data for input to machine learning procedures

***MedeA* LAMMPS:** Full access to the LAMMPS Code via a graphical user interface based on flowcharts to perform forcefield calculations using MLPs generated by *MedeA* MLPG

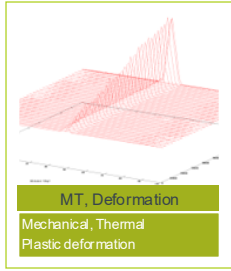

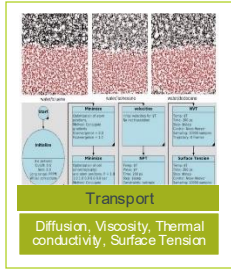

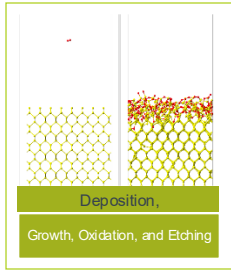

materials design

MLPs with *MedeA* LAMMPS

***MedeA* MT:** Elastic, mechanical and thermodynamic properties (also at finite temperature)

***MedeA* Deformation:** Perform deformation beyond the elastic regime

***MedeA* Thermal Conductivity:** Calculate lattice thermal conductivity with Green-Kubo or non-equilibrium MD Müller-Plathe

***MedeA* Viscosity:** Calculate viscosity with Green-Kubo or non-equilibrium MD Müller-Plathe

***MedeA* Surface Tension:** Calculate surface tension of fluid slabs

***MedeA* Diffusion:** Automatically calculate diffusivity from mean square displacement

***MedeA* Deposition:** Atomistic scale simulation to study deposition, growth, oxidation and etching

***MedeA* Phonon:** Phonon spectra and thermodynamic functions (vibrational free energy, heat capacities)

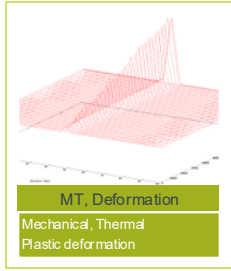

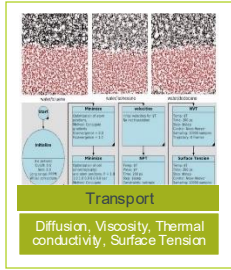

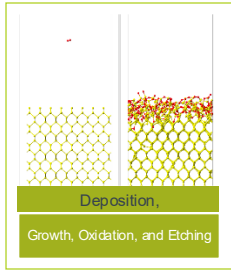

materials design